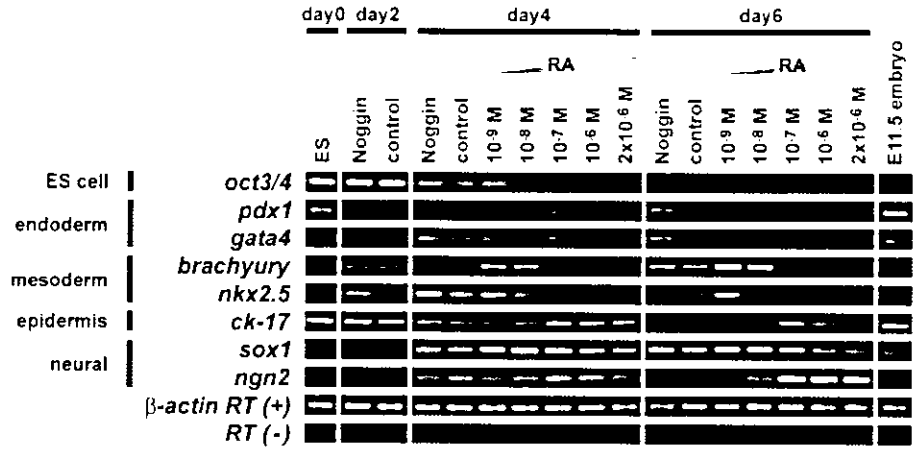

Fig. 2. Expression of markers of the three primary germ layers in EBs exposed to various concentrations of RA. RNA was isolated from ES cells (day 0) and EBs (days 2, 4, 6) and analyzed by RT-PCR for expression of markers of undifferentiated ES cells (*oct3/4*), endoderm differentiation (*pdx1* and *gata4*), mesoderm differentiation (*brachyury* and *nkx2.5*), epidermis differentiation (*ck-17*), and neural differentiation (*sox1* and *ngn2*). To normalize their expression to the amount of cDNA present in the sample, the cDNA for endogenous *β-actin* was amplified.

expressed unstably at low levels, and their levels correlated poorly with the concentrations of RA.

Neural induction of mouse ES cells by RA

It has been shown that neural differentiation of ES cells can be promoted by RA, especially by early exposure of EBs to relatively high RA concentrations (Bain et al., 1995, 1996; Fraichard et al., 1995; Gajovic et al., 1997; Renoncourt et al., 1998; Rohwedel et al., 1999; Strubing et al., 1995; Wichterle et al., 2002). However, as the effect of different RA concentrations had never been precisely described, we next investigated how RA promotes neural differentiation. EBs that had been cultured for 6 days were analyzed for differentiation markers of neural cells (progenitors, neurons, and glia) by Western blotting (Figs. 3A, B). Nestin, which is expressed in undifferentiated neural progenitors, was more strongly expressed in EBs treated with low-RA. Expression of βIII-tubulin and GFAP, which are markers of differentiated neurons and astrocytes, respectively, increased in a concentration-dependent manner in EBs exposed to RA (Figs. 3A, B). By contrast, RT-PCR analysis on day 6 showed that expression of *sox1* (a marker of undifferentiated neural cells; Pevny et al., 1998; Wood and Episkopou, 1999) mRNA was higher in EBs treated with low-RA on day 6 (Fig. 2). Expression of CNPase, a marker of oligodendrocytes, was detected only slightly under all of the differentiating conditions, and its expression was not very strongly affected by the concentration of RA (Figs. 3A,B). To better understand the effects of RA on neural differentiation of EBs, we performed immunocytochemistry of markers of various neural lineages (Figs. 3C–E and 5A,B). EBs that had been cultured for 6 days were dissociated and differentiated on poly-L-ornithine/fibronectin-coated cover glasses for 24 h and then processed for immunocytochemistry of markers of undifferentiated neural cells (Nestin, Group B1 Sox, Olig2) and postmitotic neurons (βIII-tubulin). Olig2 is a basic-helix-loop-helix (bHLH) transcription factor that is expressed in most of the ventral neural progenitor cells around the period of neural tube closure (Takebayashi et al., 2000). Treatment of EBs with low-RA (10^{-8} M) induced a 1.6-, 3.0-, and 9.1-fold increase in Nestin-, Group B1 Sox, and Olig2-positive undifferentiated neural progenitors, respectively, over those treated with high-RA (2×10^{-6} M) (Figs. 3C–E). Treatment of EBs with high-RA (2×10^{-6} M) induced very few Nestin-, Group B1 Sox-, and Olig2-positive progenitor cells, and instead induced many βIII-tubulin-positive postmitotic neurons [3.0-fold more than by treatment with low-RA (10^{-8} M)] (Figs. 3C–E and 5A). RT-PCR analysis showed that *olig2* was expressed in EBs treated with high-RA at day 4 and down-regulated by day 6, whereas it was expressed highly on day 6 in EBs treated with low-RA (Fig. 6A). These results indicate that higher concentrations of RA facilitate differentiation of neural progenitors into postmitotic neurons and glia, in contrast to lower concentrations of RA, which preferentially induce undifferentiated neural progenitor cells from ES cells; that is, that RA strongly promotes terminal differentiation of ES-cell-derived neural progenitors in a concentration- and culture-period-dependent manner in addition to its action that promotes neural induction of ES cells.

ES-cell-derived neural cells acquire positional identity through EB formation

To investigate how RA regulates the specification of rostro-caudal and dorso-ventral positional identity during EB formation, RT-PCR analysis of regionally specific markers was performed (Carpenter, 2002; Caspary and Anderson, 2003; Helms and Johnson, 2003; Hitoshi et al., 2002; Jessell, 2000; Marquardt and Pfaff, 2001;

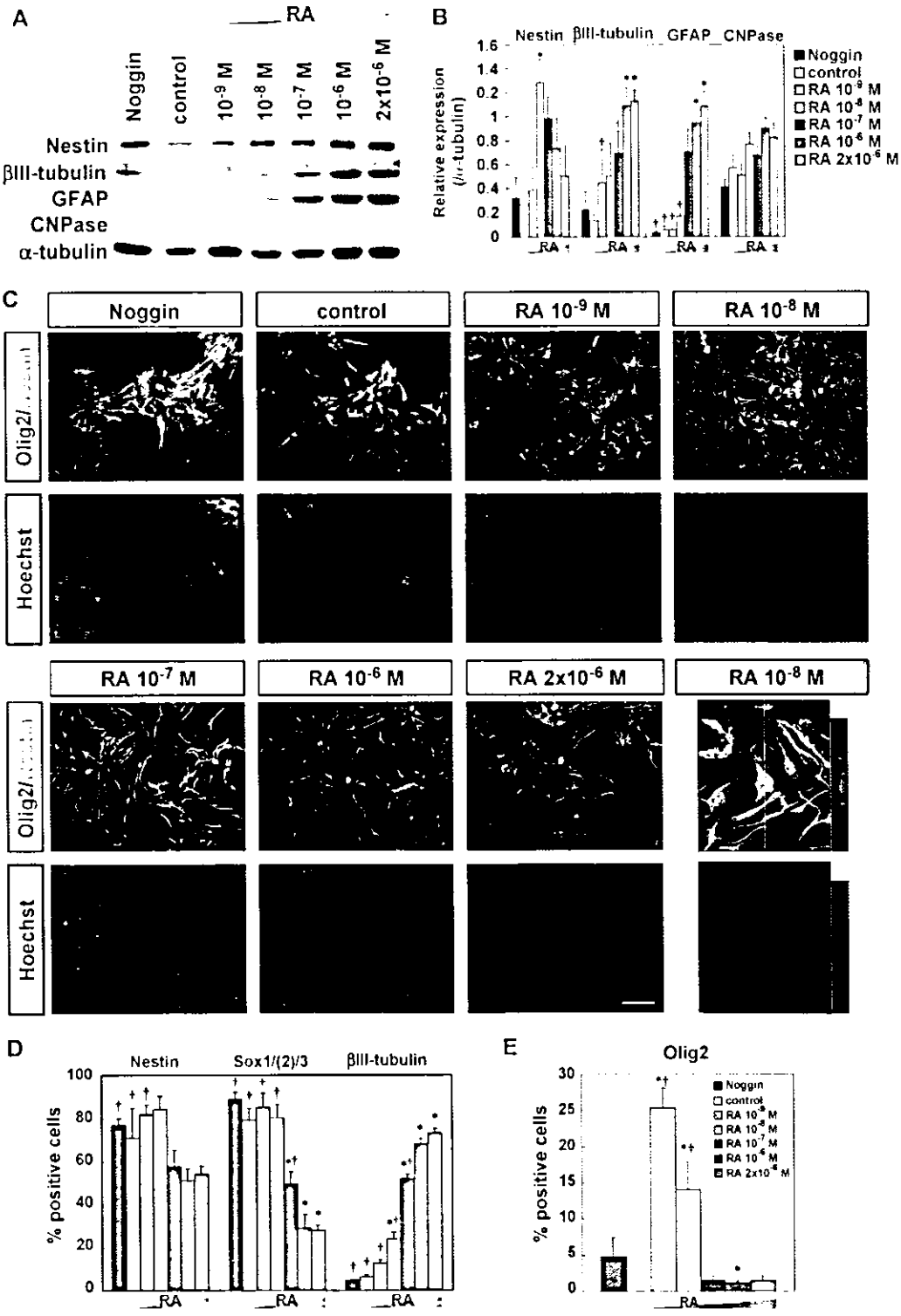

Fig. 3. RA promotes neural differentiation in a concentration-dependent manner and regulates the differentiation of ES-cell-derived neural progenitors. (A) Western blot analysis of markers for neural differentiation in EBs cultured for 6 days. (B) Quantitative analysis was performed with Scion Image. The amounts of proteins were normalized to those of α-tubulin ($n = 3$, mean ± SEM, *, $P < 0.05$ vs. control. †, $P < 0.05$ vs. RA 2×10^{-6} M). (C) Immunocytochemistry of dissociated EBs for Olig2 and Nestin. Nuclear localization of Olig2 in Nestin immunoreactive cells was confirmed by three-dimensional reconstruction of confocal microscopic images (right end of lower panels). (D, E) The proportions of cells positive for Nestin, Group B1 Sox, Olig2, and βIII-tubulin among the total number of cells in dissociated EBs were determined by immunocytochemically. Immunoreactive cells as a percentage of the total number of cells counted on the basis of nuclear staining with hoechst33342 are shown ($n = 3$, mean ± SEM, *. $P < 0.05$ vs. control. †, $P < 0.05$ vs. RA 2×10^{-6} M). The percentages of cells expressing Olig2, Group B1 Sox, and Nestin were higher in dissociates of EBs treated with low-RA ($<10^{-8}$ M) than in EBs treated with high-RA ($>10^{-7}$ M). Scale bar: 50 μm.

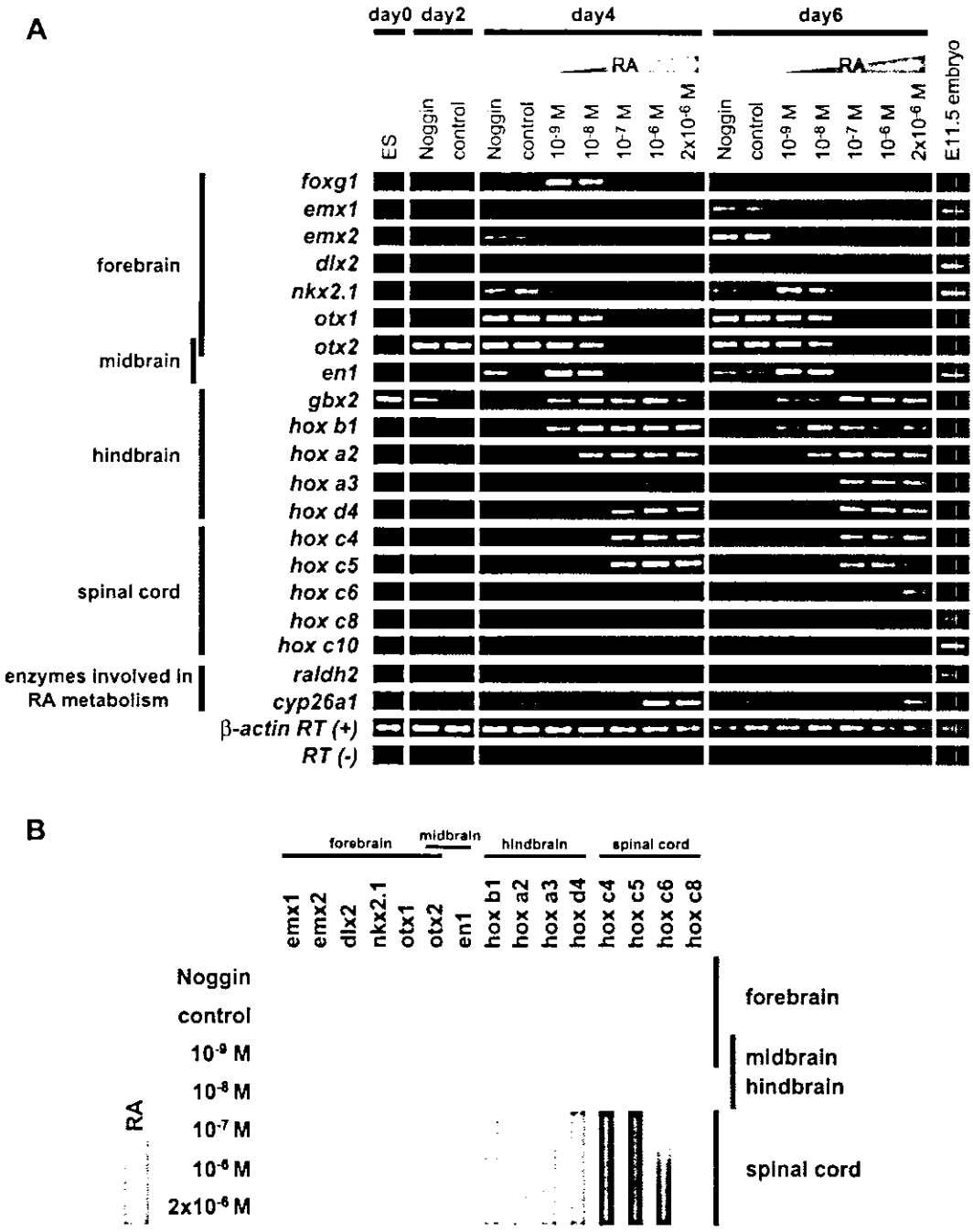

Fig. 4. Concentration-dependent effects of RA on the specification of rostrol-caudal positional identity of ES-cell-derived neural progenitors. (A) Effect of RA on rostrol-caudal axis formations was analyzed by RT-PCR on days 0, 2, 4, and 6 of differentiation. The expression patterns are summarized in (B). RA caudalized ES-cell-derived neural cells in a concentration-dependent manner. Control and Noggin-treated-EBs expressed forebrain-type markers, whereas EBs treated with low-RA and high-RA expressed midbrain–hindbrain-type markers and spinal-cord-type markers, respectively.

Fig. 5. RA caudalizes EB-derived neurons in a concentration-dependent manner. (A) Immunocytochemical analysis of neural progenitors and neurons differentiated from dissociated EBs with Otx1, which is expressed in developing forebrain and midbrain, and Phox2B, Lim3, HB9, and Isl-1/2, which are expressed in developing motor neurons and their progenitors. Immunoreactive cells as a percentage of the total number of cells counted on the basis of the nuclear staining with hoechst33342 are shown in B ($n = 3$, mean ± SEM, *, $P < 0.05$ vs. control. †, $P < 0.05$ vs. RA 2×10^{-6} M). (C) RT-PCR analysis of *phox2b* and *hb9*. Control and Noggin-treated EBs generated significant numbers of Otx1-and Group B1 Sox-positive anterior neural progenitors. Low-RA (10^{-9}–10^{-8} M) induced many Phox2b-positive hindbrain brachial and visceral motor neurons and fewer Otx1/Group B1 Sox-positive anterior neural progenitors, whereas high-RA (>10^{-7} M) induced more HB9-positive hindbrain and spinal cord somatic motor neurons without any Otx1-positive cells. Scale bar: 50 μm.

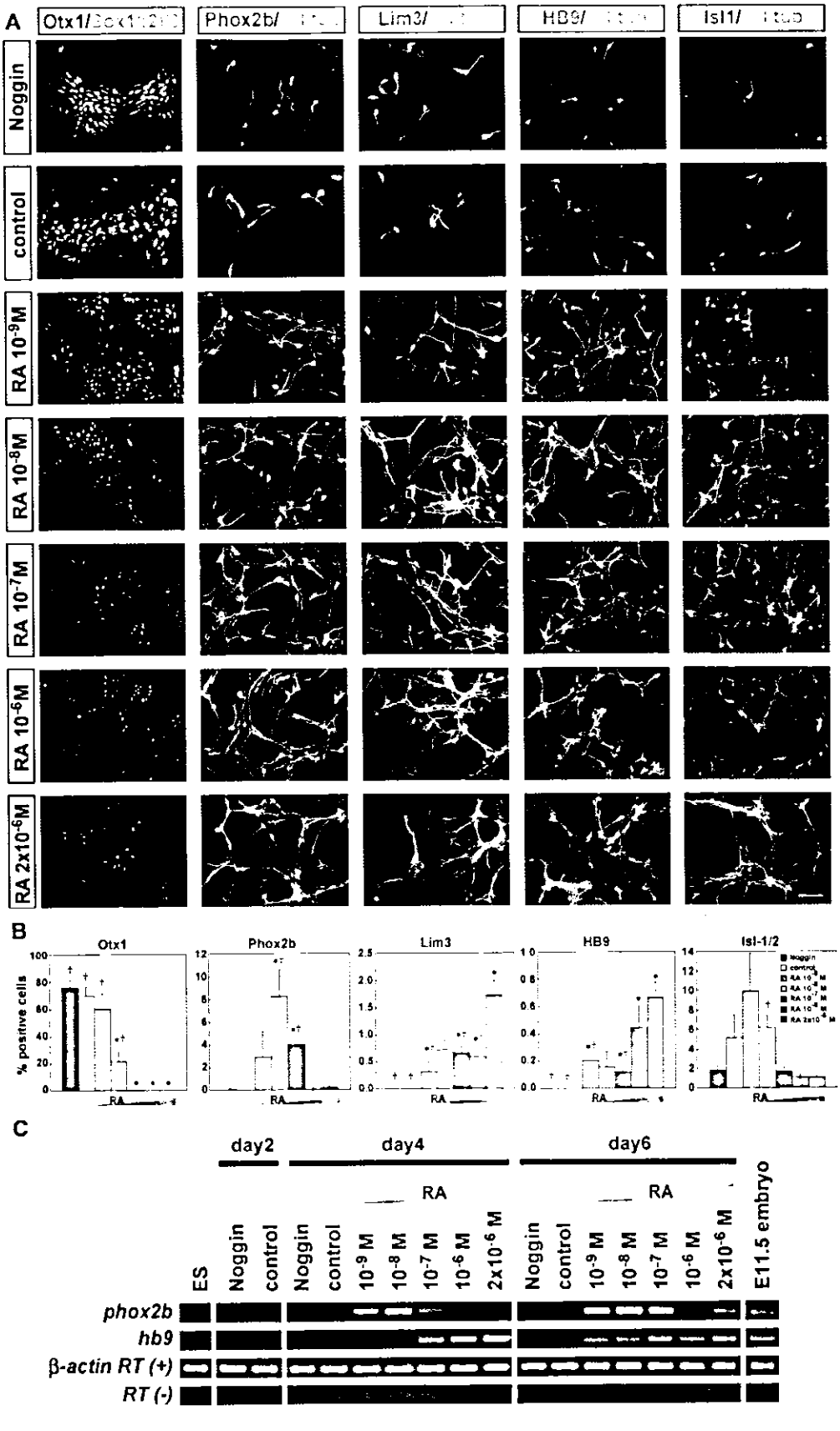
A
Otx1/
Phox2b/
Lim3/
HB9/
Isl1/
Noggin
control
RA 10-9M
RA 10-8M
RA 10-7M
RA 10-6M
RA 2x10-6M
B
Otx1
Phox2b
Lim3
HB9
Isl-1/2
% positive cells
RA
C
day2
day4
day6
RA
ES
Noggin
control
10-9 M
10-8 M
10-7 M
10-6 M
2x10-6 M
E11.5 embryo
phox2b
hb9
β-actin RT (+)
RT (-)

Niederreither et al., 2000; Schuurmans and Guillemot, 2002; Wurst and Bally-Cuif, 2001). As shown in Fig. 4, EBs were caudalized in a concentration-dependent manner during the first 2 days of RA exposure (days 2–4). After day 4, control and Noggin-exposed EBs expressed genes specific to forebrain (*emx1*, *emx2*, *nkx2.1*, *otx1*, *otx2*) and midbrain–hindbrain (*otx1*, *otx2*, *en1*), but no hindbrain or spinal cord markers. EBs treated with low-RA mainly expressed midbrain–hindbrain markers (*otx1*, *otx2*, *en1*, *gbx2*, *hoxb1*, *hoxa2*, *hoxa3*), and did not express spinal cord markers (*hoxc4*, *hoxc5*, *hoxc6*, *hoxc8*, *hoxc10*). Expression of telencephalic markers (*emx1*, *emx2*, *dlx2*) in EBs treated with low-RA was lower than in control and Noggin-exposed EBs. However, at day 4, expression of one of the telencephalic markers, *foxg1*, was somehow highest in the EBs exposed to low-RA. On the other hand, high-RA induced expression of hindbrain and rostral spinal cord markers (*hoxc4*, *hoxc5*, *hoxc6*) and reduced expression of forebrain and midbrain markers. These patterns of gene expression were detected at day 4 and were maintained thereafter. The expression levels of enzymes involved in RA metabolism, *raldh2* and *cyp26a1* (Fig. 4A), were higher in EBs treated with high-RA, a finding that was consistent with the EBs exposed to high-RA acquiring the identity of rostral spinal cord, where the concentration of RA and the expression level of its synthesizing enzyme Raldh2 are the highest in the developing CNS (Swindell et al., 1999). The RA catabolizing enzyme Cyp26a1 may have been induced by high-RA as part of a negative feedback mechanism. The total gene expression patterns indicating rostro-caudal specification in EBs differentiated under different conditions are summarized in Fig. 4B. The concentration-dependent caudalization of EBs by RA treatment shown by the result of the RT-PCR analysis was confirmed by immunocytochemistry of dissociated EBs with antibodies for markers expressed in developing forebrain and midbrain (Otx1) (Acampora et al., 1998), visceral or brachial motor neurons in the hindbrain (Phox2b) (Pattyn et al., 2000), and somatic spinal motor neurons (HB9, Lim3) (Arber et al., 1999) (Figs. 5A,B). Virtually all of the marker-positive cells were also positive for either a neural progenitor marker Group B1 Sox, or pan-neuronal marker βIII-tubulin. A significant number of cells derived from EBs and grown under all conditions expressed Isl-1/2, a marker of postmitotic cholinergic neurons, including not only spinal motor neurons but those in ventral forebrain (Kohtz et al., 2001; Wang and Liu, 2001). Somatic motor neurons of the hindbrain and spinal cord expressing Lim3 and HB9 were found more frequently when treated with high-RA, whereas hindbrain visceral or brachial motor neurons expressing Phox2b were found more frequently when treated with low-RA. By contrast, an enormous number of neural progenitors that were positive for both Otx1 and Group B1 Sox and acquired anterior positional identity were induced from control and Noggin-treated EBs, and less frequently from low-RA treated EBs, whereas no such cells were induced from high-RA-treated EBs. Taken together, these findings indicate that RA induced both caudalization of EBs based on the expression patterns of regionally specific genes during neural induction and neuronal differentiation in a concentration-dependent manner, resulting in significant generation of forebrain and midbrain (control and Noggin), hindbrain (low-RA), and spinal cord (high-RA) types of neural progenitors or neurons, respectively.

RA controls dorso-ventral axis formation

To determine the effect of RA on dorso-ventral axis specification of EB-derived cells, we investigated the expression of class I genes (*pax7*, *dbx1*, *dbx2*, *irx3*, *pax6*, whose expression is *repressed* by Shh in early CNS development) and class II genes (*nkx6.2*, *nkx6.1*, *olig2*, *nkx2.2*, whose expression is *activated* by Shh). These genes are differentially expressed along the dorso-ventral axis in the progenitor domains of developing hindbrain and spinal cord (Jessell, 2000). As shown in Fig. 6, EBs treated with low-RA expressed both class I and class II genes, indicating that they were composed of various populations that had acquired their identities throughout the dorsal to ventral neural tube. Interestingly, on the other hand, treatment with high-RA raised the expression levels of class I genes and significantly reduced those of class II genes except *olig2* at day 4, in comparison to treatment with low-RA. Thus, high-RA caused dorsalization of neural progenitor cells in EBs. To investigate the mechanism underlying the action of RA in specifying dorso-ventral identity, we investigated its effects on expression of the N-terminus of Shh protein (Shh-N) and *sonic hedgehog* (*shh*) mRNA. Mouse Shh is produced as a 49-kDa secreted protein that post-translationally cleaves to yield two mature proteins: an approximately 19-kDa N-terminal fragment that contains the signaling portion of the molecule and an approximately 27-kDa C-terminal fragment, which has auto-processing activity (Marti et al., 1995; Porter et al., 1995, 1996; Roelink et al., 1995). We found that expression of both the Shh-N protein and *shh* mRNA was significantly up-regulated by exposure to low-RA in day 4–6 EBs (Figs. 7A–C), but that further increasing the RA concentration ($>10^{-7}$ M) induced their down-regulation instead. More specifically, the RA-responsive increase in Shh-N expression appeared to be concentration-dependent up to 10^{-8} M, but was completely abrogated at 10^{-7} M and higher concentrations. On the other hand, the peak level of full-length Shh protein expressed in response to exposure to 10^{-8} M of RA was maintained even in EBs exposed to higher concentrations of RA. These results suggested that the ventralization of neural progenitors in EBs exposed to low-RA might be caused by an enhanced expression of Shh-N. However, we

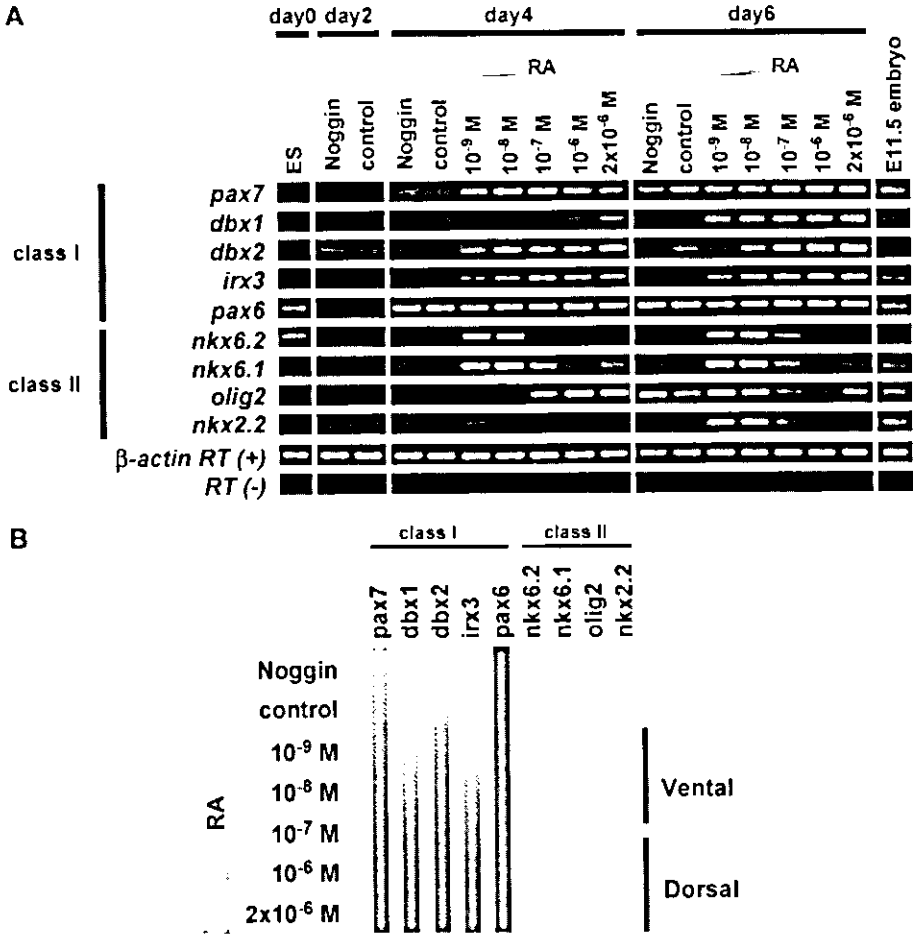

Fig. 6. Specification of the dorso-ventral identity of ES-cell-derived neural progenitors is regulated by RA. (A) RT-PCR analysis of class I and class II genes, which define dorsol-ventral positional identity. The expression patterns are summarized in (B). EBs treated with low-RA (10^{-9}–10^{-8} M) expressed both class I and II genes (class II > class I), which indicated that both ventral and dorsal neural progenitors had been induced, whereas EBs treated with high-RA (>10^{-6} M) expressed only class I gene, indicating dorsal neural progenitors had been induced.

could not rule out the possibility of the opposite causal relationship; that is, that low-RA induced enhanced expression of Shh-N protein and the expression of *shh* mRNA resulted from the ventralization of EB-derived cells that had been induced by low-RA treatment through an unknown mechanism. To address this issue, we treated EBs exposed to RA with recombinant Shh-N protein and cyclopamine, an inhibitor of Shh signaling (Chen et al., 2002a,b; Incardona et al., 1998). In the absence of cyclopamine treatment, EBs exposed to low-RA expressed both class I (*pax7*, *dbx1*, *dbx2*, *irx3*, and *pax6*) and class II genes (*nkx6.2*, *nkx6.1*, *olig2*, and *nkx2.2*), thereby indicating both dorsal and ventral phenotype. Treatment with 1 μM cyclopamine strongly down-regulated the ventral class II genes (*nkx6.2*, *nkx6.1*, *olig2*, and *nkx2.2*) and some of the class I genes (*dbx1* and *dbx2*), indicating a dorsalized phenotype (Figs. 7D,E). In addition, exposure to 50 nM of recombinant Shh-N protein enhanced expression of class II genes (*nkx6.2*, *nkx6.1*, *olig2*, and *nkx2.2*) but reduced *pax7* expression. These effects were abrogated by treatment with 1 μM cyclopamine (Figs. 7D,E). EBs treated with high-RA expressed higher levels of class I genes (*pax7*, *dbx1*, and *dbx2*, *irx3*, *pax6*), but lower levels of class II genes (*nkx6.2*, *nkx6.1*, *olig2*, and *nkx2.2*), thereby indicating a more dorsal phenotype than after low-RA treatment. However, high-RA treated EBs were ventralized by treatment with exogenous Shh-N, as shown by the up-regulation of class II genes (*nkx6.2*, *nkx6.1*, *olig2*, and *nkx2.2*) and down-regulation of *pax7*, and these changes were also abrogated by 1 μM cyclopamine treatment (Figs. 7D,E).

This alteration of dorso-ventral identity by RA, Shh-N, and cyclopamine was confirmed by the immunostaining of dissociated EBs with antibodies against Pax7, Nkx6.1, and Nkx2.2 (Fig. 8). Virtually all the marker-positive cells also stained with the antibodies against Group B1 Sox or Nestin, indicating they are neural progenitor cells. It was noteworthy that Shh-N treatment could induce only Nkx6.1-positive but not Nkx2.2-positive neural progenitors in EBs treated with high-RA, indicating that the ventralmost neural progenitors could not be efficiently derived under such conditions, but that they were capable of increasing the

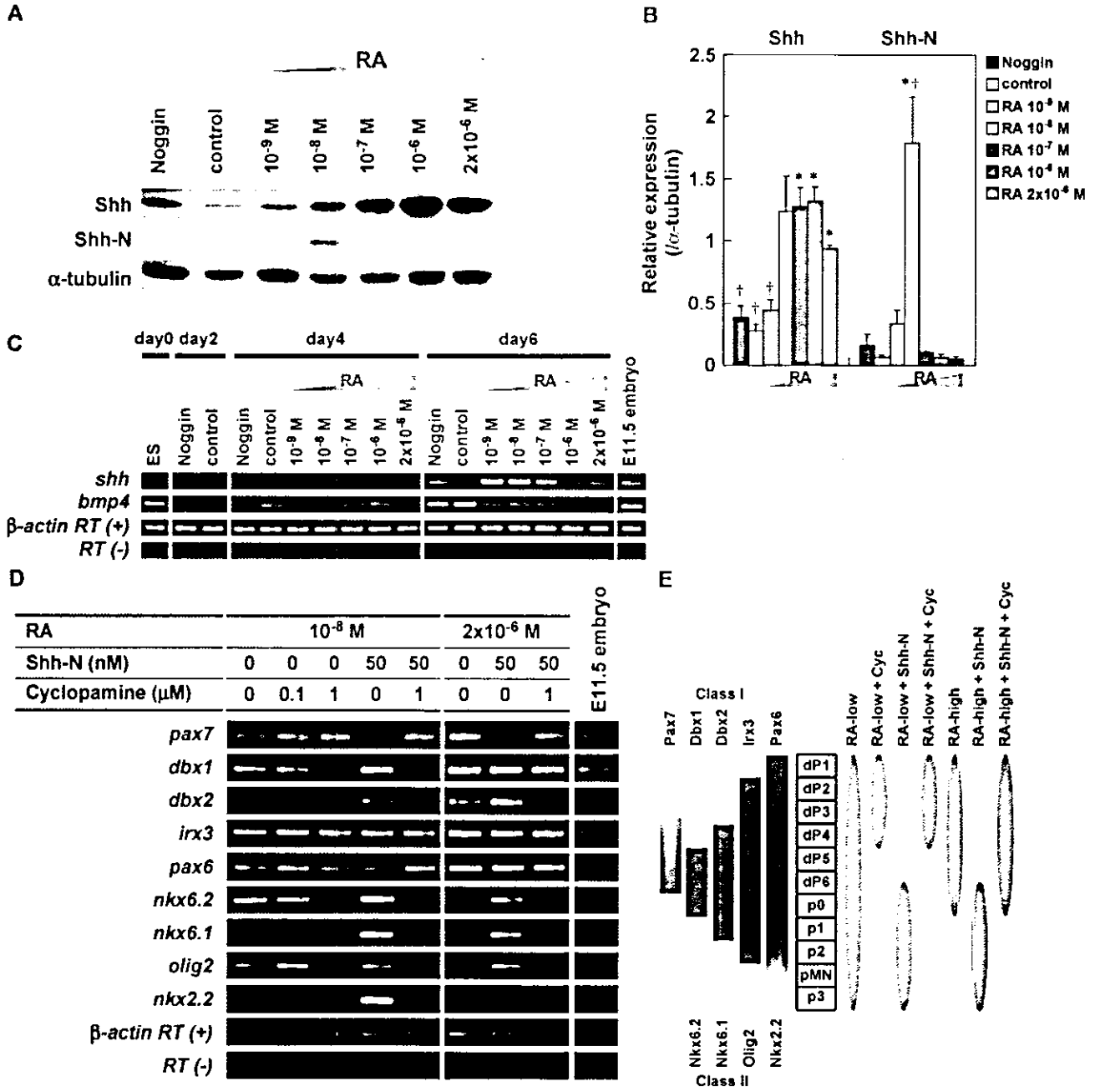

Fig. 7. Shh-N mediates RA-dependent dorso-ventral specification of ES-cell-derived neural progenitors. (A) Expression of Shh and its active N-terminal truncated form, Shh-N, in EBs cultured for 6 days, was analyzed by Western blotting. EBs were exposed to various concentrations of RA. Quantitative analysis was performed with Scion Image. The amounts of proteins were normalized to those of α-tubulin (B) ($n = 3$, mean ± SEM, *, $P < 0.05$ vs. control. †, $P < 0.05$ vs. RA 2×10^{-6} M). (C) RT-PCR analysis of *shh* and *bmp4*. Shh-N was more highly expressed in EBs treated with low-RA (10^{-9} M–10^{-8} M). (D) RT-PCR analysis of RA-exposed EBs treated with Shh-N and its inhibitor cyclopamine. Shh-N and cyclopamine were added together with RA on day 2. (E) Summary of expression patterns in vitro corresponding to in vivo. Cells from low-RA-treated EBs were a mixed population of dorsal-to-ventral neural progenitors and were capable of being dorsalized by inhibiting Shh signaling with cyclopamine. By contrast, exogenous Shh-N induced ventral neural progenitors were capable of being dorsalized by cyclopamine. Cells from high-RA-treated EBs showed dorsal positional identities. However, addition of Shh-N increased the number of ventral neural progenitors, and they were also capable of being dorsalized by cyclopamine treatment.

Fig 8. Dorso-ventral specification of RA treated EBs is altered by Shh-N and cyclopamine. The alteration of dorso-ventral identity by RA, Shh-N, and cyclopamine was confirmed by the immunostaining of dissociated EBs with antibodies against Pax7 as a marker for dorsal neural progenitors, against Nkx6.1 as a marker for ventral neural progenitors, and against Nkx2.2 as a marker for ventralmost neural progenitors in combination with Group B1 Sox or Nestin as a marker for neural progenitors. Immunoreactive cells as a percentage of the total number of cells counted on the basis of the nuclear staining with hoechst33342 are shown in B ($n = 3$, mean ± SEM). Scale bar: 50 μm.

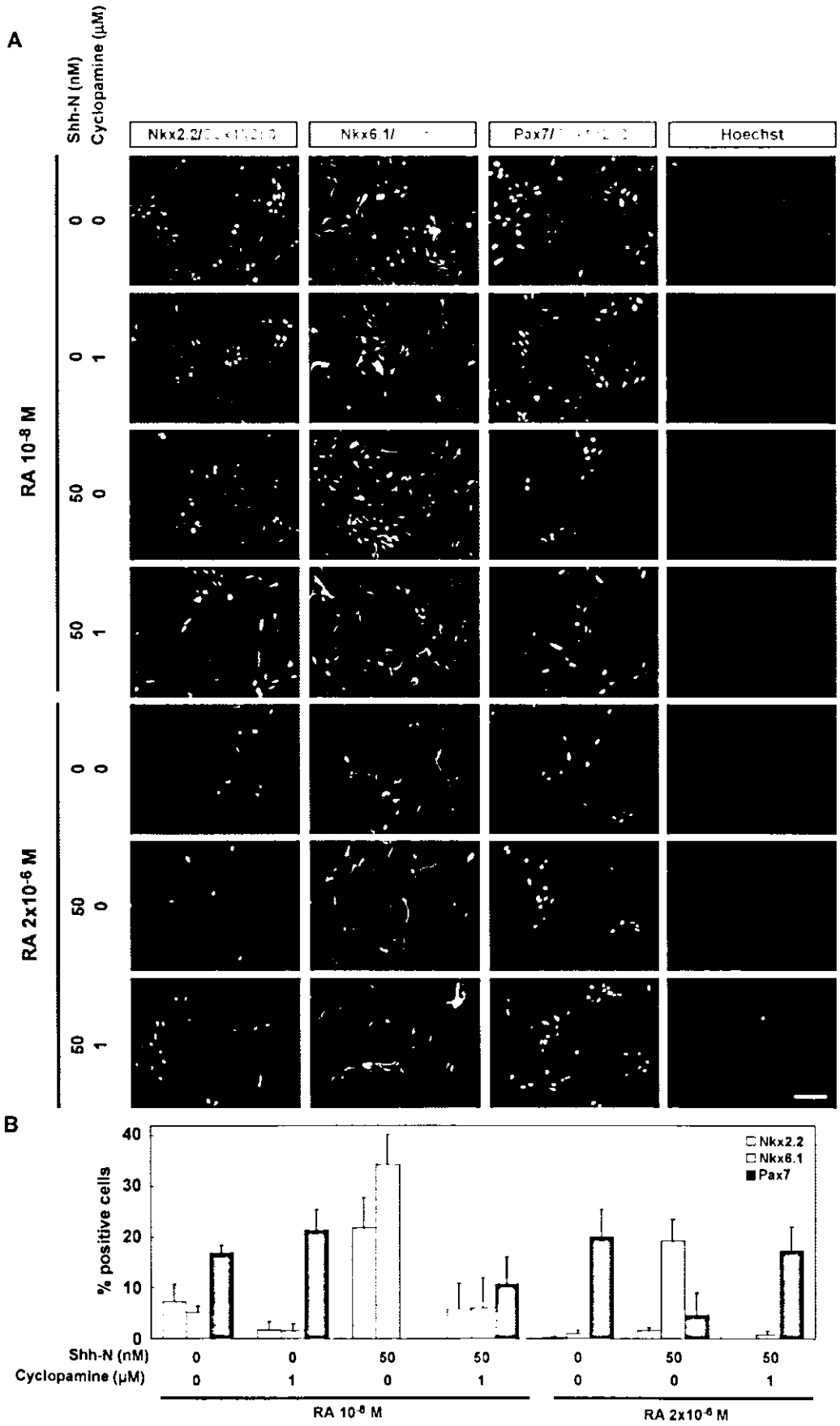
A
Shh-N (nM)
Cyclopamine (μM)
Nkx2.2/
Nkx6.1/
Pax7/
Hoechst
RA 10-8 M
RA 2x10-6 M
0
0
0
1
50
0
50
1
B
% positive cells
40
30
20
10
0
Nkx2.2
Nkx6.1
Pax7
Shh-N (nM) 0 0 50 50 0 50 50
Cyclopamine (μM) 0 1 0 1 0 0 1
RA 10-8 M
RA 2x10-6 M

number of Nkx6.1- or Nkx2.2-positive ventral neural progenitors in EBs treated with low-RA. The observation in EBs treated with high-RA is consistent with the previous report (Wichterle et al., 2002).

One of the major dorsalizing molecules in the CNS, *bmp4* (Caspary and Anderson, 2003; Jessell, 2000; Knecht and Bronner-Fraser, 2002), was not very strongly affected by RA, Shh-N, or cyclopamine, suggesting a lesser contribution of the BMP signal to this RA-mediated dorso-ventral specification (Fig. 7C, data not shown). These results indicate that differentiating EBs were ventralized by low-RA through induction of endogenous Shh-N protein, and that the effect was abrogated by cyclopamine and enhanced by the addition of exogenous Shh signal (Figs. 7D,E and 8).

Positional identity regulated by the RA concentration is mainly determined during the first 2 days of exposure to RA

According to the RT-PCR analysis of EBs cultured according to the 2−/4+ protocol, the expression patterns of most of the regionally specific markers were determined by day 4 and maintained unchanged thereafter. This observation raised two possibilities. One possibility is that the first 2 days of exposure to RA are critical to the determination of positional identity, and the second is that the effect of the RA concentration was altered during the later culture period by degradation of RA. To determine which of these possibilities was true, we performed a RT-PCR analysis of EBs cultured according to other protocols in which the times when RA is added or the duration of exposure to RA (2−/2+/2−, 2−/2+/2+, and 4−/4+ protocols) is different from the 2−/4+ protocol (Suppl. Fig. 1). Expression of *oct3/4* had been maintained before the addition of RA, but no expression of other markers except *otx2*, whose mRNA was expressed even in undifferentiated ES cells, had been detected in any of the culture protocols, including the 4−/4+ protocol. The expression patterns of most of regionally specific markers were determined by day 4 of the 2−/2+/2− and 2−/2+/2+ or by day 6 of the 4−/4+ protocol, and were virtually the same in all protocols as observed in the 2−/4+ protocol, and they were maintained thereafter as well (Suppl. Fig. 2). Overall, positional identity is determined during the first 2 days of exposure to RA and is maintained thereafter regardless of the presence or absence of RA in later culture periods.

Discussion

The pluripotent embryonic stem cell is a valuable in vitro model for studying the effects of various factors on cell lineage decisions in very early embryonic stages of mammalian development, and the effect of RA signaling on the differentiation of ES cells and neural induction, in particular, has been extensively studied. In addition to previous reports showing that RA promotes neural differentiation of ES cells and caudalization of the positional identity of their progeny (Bain et al., 1995, 1996; Fraichard et al., 1995; Gajovic et al., 1997; Renoncourt et al., 1998; Strubing et al., 1995; Wichterle et al., 2002), the results of the present study demonstrate the novel and precise actions of RA on neural differentiation and acquisition of positional identity by ES-cell-derived neural cells.

Effect of the concentration of RA on ES cell differentiation

It is well known that exposure of growing EBs to high-RA markedly increases the rate of neural differentiation, whereas low-RA induces more mesodermal cells (Rohwedel et al., 1999). Higher concentrations of RA also promote faster differentiation of ES cells, as indicated by the pattern of *oct3/4* expression, which was down-regulated more rapidly in EBs exposed to higher concentrations of RA, and down-regulated more at day 6 than at day 4 (Fig. 2). The result of this study showed that RA also concentration-dependently facilitates terminal differentiation of neural cells derived from ES cells. The expression levels of markers of differentiated neurons and glia, i.e., of βIII-tubulin and GFAP, respectively, was higher in EBs treated with higher concentrations of RA, whereas the expression levels of markers of undifferentiated neural cells, i.e., of Nestin, Group B1 Sox, Olig2, and *sox1* mRNA, was inversely correlated with the concentration of RA (Figs. 2 and 3). The findings are consistent with a high-RA enhancing differentiation of neural progenitor cells, as described previously (Bain et al., 1995, 1996; Fraichard et al., 1995; Gajovic et al., 1997; Renoncourt et al., 1998; Strubing et al., 1995; Wichterle et al., 2002).

Down-regulation of Wnt signaling has been shown to be one of the mechanisms involved in RA-induced neural differentiation of mouse ES cells (Aubert et al., 2002). Interestingly, β-catenin, which is a key molecule in Wnt signaling, has been shown to interact directly with retinoid receptor RAR, but not with RXR, in a retinoid-dependent manner, and as a result retinoids decrease β-catenin-Lef/Tcf-mediated transactivation in cultured cells in a dose-dependent manner (Easwaran et al., 1999). Wnt3a signaling through Lef/Tcf1 has also been implicated in suppression of neural differentiation and induction of mesodermal differentiation in the mouse embryo (Galceran et al., 1999; Yamaguchi et al., 1999; Yoshikawa et al., 1997). These findings raise the possibility that the one of the effects of RA in EBs is to inhibit the Wnt-β-catenin anti-neural pathway by up-regulation of Secreted frizzled-related protein 2 (Sfrp2) (Aubert et al., 2002) and/or sequestration of β-catenin in a concentration-dependent manner, thereby resulting in the promotion of neural differentiation, and inversely in the suppression of mesodermal differentiation.

FGFs are another molecules that may be involved in the neurogenesis related to RA signaling. RA has been shown to promote neuronal differentiation by repressing FGF signalings from the posterior neural plate. Caudal FGF signalings

have the opposite effects and repress Raldh2 (RA synthesis) in the presomatic mesoderm and generic neuronal differentiation in chick early neural tube (Diez del Corral et al., 2003; Novitch et al., 2003). These observations raise the possibility that RA inhibits the action of endogenously generated FGFs in a concentration-dependent manner during the culture of EBs. Further study of the associations between these signals is required to clarify the mechanism underlying the RA-promoted neural differentiation of ES cells.

Acquisition of rostro-caudal identity depends on the concentration of RA

A previous study on chick embryos showed that the default identity of early neural tissue is a rostral location and that neural cells can be caudalized by exogenous factors, such as the caudalizing activity of paraxial mesoderm, FGFs, and retinoid from the mesoderm, which induce midbrain, hindbrain, and spinal cord characters, when applied during the appropriate period of development (Muhr et al., 1999).

RA is one of the factors, that has been shown to be involved in hindbrain patterning and the caudalization of neural tissues in the early embryonic CNS in vivo (Maden, 2002). The distribution of endogenous RA has been examined in mouse and chick embryos, by various method, including HPLC (high-performance liquid chromatography) (Horton and Maden, 1995; Maden et al., 1998), the use of *LacZ* reporter cells (Maden et al., 1998; Wagner et al., 1992), and the use of RARβ_2-*LacZ* transgenic mice (Reynolds et al., 1991; Zimmer, 1992). This distribution of endogenous RA is correlated with the opposing action of the two main enzymes involved in RA-metabolism, RA-synthesizing enzyme, Raldh2, which is most strongly expressed in the paraxial mesoderm adjacent to the rostral spinal cord with the rostral boundary of the presumptive first somite (Berggren et al., 1999), and the catabolizing enzyme, Cyp26a1, which is expressed in anterior neuroepithelium. These spatially distributed enzymes create a rostro-caudal RA concentration gradient in vivo (Abu-Abed et al., 2001; Fujii et al., 1997; Maden et al., 1998; Sakai et al., 2001; Swindell et al., 1999), with the peak RA concentration occurring at the hindbrain/spinal cord boundary, with levels gradually decreasing anterior and posterior to it. Furthermore, it has been suggested that the patterning of the rhombomere is influenced over time by the constant supply of RA from the paraxial mesoderm, where the neuroepithelium grows and moves away form this source of RA. These findings imply that the more posterior rhombomeres that develop later than the more anterior rhombomeres may have been exposed to higher concentration of RA, leading to the expression of more posterior genes (such as posterior *hox* genes), which require a higher concentration of RA for activation in vivo (Maden, 2002). Our findings are consistent with the above-described putative regulatory mechanism of hindbrain/rostral spinal cord positional specification correlated with the RA concentration gradient in vivo in the following manner. The default positional identity of ES-cell-derived neural cells is specified as anteriormost forebrain, which was acquired in the control and Noggin-exposed EBs. EBs treated with low-RA were specified as midbrain to hindbrain, which is generated earlier and require lower concentrations of RA in vivo, whereas EBs treated with high-RA were specified as posterior hindbrain to rostral spinal cord, which is generated later and requires higher concentrations of RA in vivo. In addition, the fact that even the EBs treated with high-RA expressed genes specific to rostral (*hoxc4* to *hoxc6*), but not to caudal spinal cord (*hoxc8* to *hoxc10*) is consistent with the putative gradient of endogenous RA in vivo with a higher concentration in the rostral spinal cord, and the proposed role of RA in rostral spinal cord determination (Liu et al., 2001). Moreover, other factors may be involved in the activation of RA-responsive genes and the specification of positional identity, such as RA binding proteins, including cellular retinoic acid binding protein (CRABP) 1, which limits the access of RA to the nuclear retinoid receptors. The spatiotemporal pattern of expression of CRABP1 suggests that the fine regional control of availability of RA to the nuclear receptors may also play an important role in the organization of the central nervous system and the differentiation of its progenitors in vivo (Leonard et al., 1995; Maden, 2001; Maden et al., 1992; Ruberte et al., 1993). The role of these RA binding proteins in the regulation of in vitro differentiation of ES-cell-derived neural cells should be investigated further in the future.

RA also affects dorso-ventral positional identity

In contrast to the acquisition of rostro-caudal identity, dorso-ventral identity was analyzed in terms of expression of the transcriptional control of the homeodomain (HD) and basic helix-loop-helix (bHLH) proteins. Previous studies have emphasized the role of Shh signaling in establishing the pattern of expression of ventral spinal cord patterning genes (Jessell, 2000). RA has also been reported to contribute to the ventral patterning of the spinal cord; that is, to the induction of ventral interneurons (V0 and V1) by inducing class I genes, including Dbx1, Dbx2, Evx1, Evx2, and En (Pierani et al., 1999), and to the specification of limb level motor neuron subtypes by the expression of Raldh2 in LMC (Sockanathan and Jessell, 1998). Furthermore, recent studies have revealed involvement of RA from the paraxial mesoderm in the timing of neurogenesis and the patterning of the ventral spinal cord regulating the expression of class I and class II genes via inhibition of FGF signals and in combination with Shh signals (Diez del Corral et al., 2003; Novitch et al., 2003). However, the results of our study showed that the concentration of RA to which EBs were exposed was critical for acquisition of dorso-ventral identity by differentiating ES cells, and the concentration dependency showed a bell-

shaped pattern. This was shown by the pattern of the expression of class I and class II genes (Figs. 6A,B), which determines the dorso-ventral progenitor domains of developing hindbrain and spinal cord. EBs exposed to high-RA exhibit mainly dorsal phenotypes, whereas EBs exposed to low-RA exhibit more ventral phenotypes (Figs. 6–8). The expression pattern of *olig2*, higher at day 4 in EBs treated with high-RA and at day 6 in those treated with low-RA, seems to conflict with this finding; however, there are several possible explanations. One is that this alteration of the expression pattern of *olig2* mimics that in vivo according to the stage of development, with expression in most of the undifferentiated neural/glial progenitor cells in the ventral half of the spinal cord occurring around the period of neural tube closure and later being restricted to the motor neuron domain (pMN domain) of the ventral ventricular region, where the progenitors of motor neurons and oligodendrocytes arise sequentially (Lu et al., 2000; Takebayashi et al., 2000; Zhou et al., 2001). Thus, both the cells collected at day 4 from EBs exposed to high-RA and those collected at day 6 from EBs exposed to low-RA may consist of multipotent neural progenitors expressing Olig2. Furthermore, the role of RA in motor neuron development, such as its effect on the expression of bHLH and HD transcription factors, including Olig2, varies with the stage of development, according to a previous study that analyzed chick spinal cord development (Novitch et al., 2003). Similar alteration of the effects of RA may occur in our culture system and be another possible explanation for the sequential expression pattern of *olig2* in EBs exposed to high-RA.

The ventralization of EBs treated with low-RA can be explained by the finding that the active form of Shh-N, which is secreted by the notochord and floor plate of the developing CNS and ventralizes gene expression of neural progenitors in a concentration-dependent manner in vivo (Jessell, 2000), is more highly expressed on day 6 in EBs treated with low-RA (Figs. 7A–C). The hypothesis that the concentration-dependent activity of RA that defines dorso-ventral identity is mediated by Shh-N was confirmed by the result of treatment with the inhibitor of Shh signaling, cyclopamine (Figs. 7D,E and 8) (Chen et al., 2002a,b; Incardona et al., 1998). Cyclopamine abrogated the ventralization activity of low-RA treatment, and addition of exogenous Shh-N more efficiently ventralized differentiating EB-derived cells that had been exposed to both low-RA and high-RA, in a cyclopamine-sensitive manner. The expression level of *bmp4*, which dorsalizes neural progenitor cells (Caspary and Anderson, 2003; Jessell, 2000; Knecht and Bronner-Fraser, 2002), was not very strongly affected by Shh-N or cyclopamine in EBs exposed to either low-RA or high-RA (Fig 7C, data not shown), indicating that BMP signaling is not the major contributor to RA-mediated dorso-ventral specification. Taken together, these findings suggest that Shh-N expressed in EBs exposed to low-RA may be one of the major signals that ventralize neural progenitors and induce expression of class II genes in addition to class I genes, and that the lack of the shh signal in EBs exposed to high-RA may result in expression of only class I genes and a more dorsalized phenotype, which can be ventralized by exogenous Shh-N protein. The results of this study are consistent with a previous report that RA enhances expression of class I genes, but not of class II genes, in developing chick spinal cord (Diez del Corral et al., 2003; Novitch et al., 2003), and that exogenous Shh-N is required in addition to high-RA for efficient generation of motor neurons during EB formation in vitro (Renoncourt et al., 1998; Wichterle et al., 2002). Because EBs exposed to low-RA are mixed populations and contain many mesodermal cells (Fig. 2) (Rohwedel et al., 1999), they may secrete larger amounts of Shh-N than EBs treated with high-RA, which contain smaller proportions of mesodermal cells.

The discrepancy in response to RA between full-length Shh expression and Shh-N expressions detected by Western blotting (Figs. 7A,B) may be another important finding in this study. In contrast to the expression of full-length Shh being observed in EBs treated with RA at concentration 10^{-8} M and above, generation of Shh-N was detected only in EBs exposed to lower concentrations of RA (Figs. 7A,B), indicating the possible existence of RA-dependent machinery controlling Shh-N production by modulating an auto-processing mechanism by the C-terminus of Shh, which processes full-length Shh into the N-terminus active form, or by altering degradation activity of Shh-N.

Use of mutant ES cells for *indian hedgehog (ihh)* and *smoothened (smo)* has shown that hedgehog signaling is also required for neural differentiation of mouse ES cells by RA (Maye et al., 2004). In our study, however, expression of Group B1 Sox and *sox1* mRNA in EBs treated with low- or high-RA and their dissociates were not down-regulated by cyclopamine (Fig. 8, data not shown), indicating that neural differentiation was not inhibited under our culture conditions even in the presence of cyclopamine. There are two possible explanations for this discrepancy. In our experiments, cyclopamine was added on day 2 after the start of ES cells differentiation, whereas in the mutant ES cells in which hedgehog signaling was disrupted it was disrupted at the start of differentiation, raising the possibility that hedgehog signaling may be one of the factors that is required for the initial commitment of neuroectodermal differentiation. The other possibility is that the concentration of cyclopamine used in our study may not have been adequate to completely block hedgehog signaling, and the residual signaling activity may have been sufficient for the transition of ES-cell-derived ectoderm into neuroectoderm, but not for the ventralization of neural cells.

The mechanism underlying these roles of hedgehog signals in differentiation and specification of ES-cell-derived neural cells needs to be elucidated in the future.

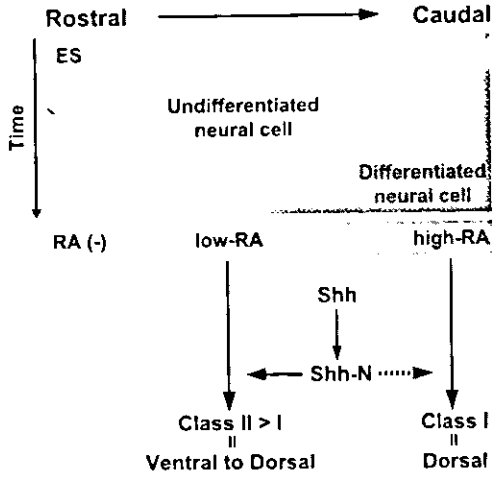

Fig 9. Schematic presentation of the concentration-dependent effects of RA on neural differentiation by mouse ES cells. RA simultaneously promotes both neural differentiation and caudalization in concentration-dependent manner. Low-RA induces a higher level of Shh-N, which endows ES-cell-derived neural progenitors with ventral identity, whereas high-RA poorly induces Shh-N, and they acquire dorsal neural identity instead.

RA is one of the most important inductive signals in vertebrate ontogeny and can be used to induce neural differentiation of mouse ES cells in vitro. However, its actions are complicated and difficult to deal with at will, because RA has the ability to induce various types of cells depending on its concentration, and it simultaneously affects both the timing of differentiation and the acquisition of positional identity, including rostro-caudal and dorso-ventral identity during neural differentiation (Fig. 9). Separation of these two phenomena is desirable to investigate the underlying mechanisms, and separation may have been accomplished, in part, by using SDIA, which is a culture protocol that induces neural cells without RA treatment. Thus, previous studies have shown involvement of RA at a single concentration in the caudalization of ES-cell-derived neural cells (Mizuseki et al., 2003; Wichterle et al., 2002). However, it is still not easy to separate these two phenomena completely during the neural induction of ES cells, because they are simultaneously affected by RA in vivo in combination with other signals, such as FGF and Shh signals, as shown by previous studies (Appel and Eisen, 2003; Diez del Corral et al., 2003; Novitch et al., 2003).

The present study identified detailed gene expression profiles and clarified the effects of the concentration of RA on ES cell differentiation, neuralization, and positional specification, though it may be impossible to map the patterns of expressions of the regional specific markers observed in ES-cell-derived neural cells directly to parallel expression of the markers in vivo. In combination with the RA-independent neural induction method using Noggin, this information will enable us to establish a strategy that will allow control of both the differentiation and the positional identity of neural cells derived from mouse ES cells through EB formation in vitro, and it may be applicable to human ES cells, raising the possibility of application to the treatment of neurological diseases.

Acknowledgments

We are grateful to Dr. H. Niwa for kindly providing ES cell line EB3, Dr. M. Nakafuku for the anti-Olig2 antibody, Dr. J.-F. Brunet for the anti-Phox2b antibody, Dr. O.D. Madsen and Dr. H. Duus for the anti-Nkx6.1 antibody, Dr. H. Kondoh for the anti-GroupB1 Sox antibody, Dr. Y. Takahashi for the xNoggin/BOS plasmid, J. Kohyama, S. Yuasa, and M. Yano for their thoughtful advice, and S. Nakamura for technical assistance. This work was supported by grants from CREST, Japan Society for the Promotion of Science to H.O.

Appendix A. Supplementary data

Supplementary data associated with this article can be found, in the online version, at doi:10.1016/j.ydbio.2004.07.038.

References

Abu-Abed, S., Dolle, P., Metzger, D., Beckett, B., Chambon, P., Petkovich, M., 2001. The retinoic acid-metabolizing enzyme, CYP26A1, is essential for normal hindbrain patterning, vertebral identity, and development of posterior structures. Genes Dev. 15, 226–240.

Acampora, D., Avantaggiato, V., Tuorto, F., Briata, P., Corte, G., Simeone, A., 1998. Visceral endoderm-restricted translation of Otx1 mediates recovery of Otx2 requirements for specification of anterior neural plate and normal gastrulation. Development 125, 5091–5104.

Appel, B., Eisen, J.S., 2003. Retinoids run rampant: multiple roles during spinal cord and motor neuron development. Neuron 40, 461–464.

Arber, S., Han, B., Mendelsohn, M., Smith, M., Jessell, T.M., Sockanathan, S., 1999. Requirement for the homeobox gene Hb9 in the consolidation of motor neuron identity. Neuron 23, 659–674.

Arceci, R., King, A., Simon, M., Orkin, S., Wilson, D., 1993. Mouse GATA-4: a retinoic acid-inducible GATA-binding transcription factor expressed in endodermally derived tissues and heart. Mol. Cell. Biol. 13, 2235–2246.

Aubert, J., Dunstan, H., Chambers, I., Smith, A., 2002. Functional gene screening in embryonic stem cells implicates Wnt antagonism in neural differentiation. Nat. Biotechnol. 20, 1240–1245.

Bain, G., Kitchens, D., Yao, M., Huettner, J.E., Gottlieb, D.I., 1995. Embryonic stem cells express neuronal properties in vitro. Dev. Biol. 168, 342–357.

Bain, G., Ray, W.J., Yao, M., Gottlieb, D.I., 1996. Retinoic acid promotes neural and represses mesodermal gene expression in mouse embryonic stem cells in culture. Biochem. Biophys. Res. Commun. 223, 691–694.

Berggren, K., McCaffery, P., Drager, U., Forehand, C.J., 1999. Differential distribution of retinoic acid synthesis in the chicken embryo as determined by immunolocalization of the retinoic acid synthetic enzyme, RALDH-2. Dev. Biol. 210, 288–304.

Blumberg, B., Bolado Jr., J., Moreno, T.A., Kintner, C., Evans, R.M.,

Papalopulu, N., 1997. An essential role for retinoid signaling in anteroposterior neural patterning. Development 124, 373–379.
Carpenter, E.M., 2002. Hox genes and spinal cord development. Dev. Neurosci. 24, 24–34.
Caspary, T., Anderson, K.V., 2003. Patterning cell types in the dorsal spinal cord: what the mouse mutants say. Nat. Rev., Neurosci. 4, 289–297.
Chen, J.K., Taipale, J., Cooper, M.K., Beachy, P.A., 2002a. Inhibition of Hedgehog signaling by direct binding of cyclopamine to Smoothened. Genes Dev. 16, 2743–2748.
Chen, J.K., Taipale, J., Young, K.E., Maiti, T., Beachy, P.A., 2002b. Small molecule modulation of Smoothened activity. Proc. Natl. Acad. Sci. 99, 14071–14076.
Diez del Corral, R., Olivera-Martinez, I., Goriely, A., Gale, E., Maden, M., Storey, K., 2003. Opposing FGF and retinoid pathways control ventral neural pattern, neuronal differentiation, and segmentation during body axis extension. Neuron 40, 65–79.
Easwaran, V., Pishvaian, M., Salimuddin, S., Byers, S., 1999. Cross-regulation of [beta]-catenin-LEF/TCF and retinoid signaling pathways. Curr. Biol. 9, 1415–1418.
Finley, M.F., Devata, S., Huettner, J.E., 1999. BMP-4 inhibits neural differentiation of murine embryonic stem cells. J. Neurobiol. 40, 271–287.
Fraichard, A., Chassande, O., Bilbaut, G., Dehay, C., Savatier, P., Samarut, J., 1995. in vitro differentiation of embryonic stem cells into glial cells and functional neurons. J. Cell Sci. 108 (Pt 10), 3181–3188.
Fujii, H., Sato, T., Kaneko, S., Gotoh, O., Fujii-Kuriyama, Y., Osawa, K., Kato, S., Hamada, H., 1997. Metabolic inactivation of retinoic acid by a novel P450 differentially expressed in developing mouse embryos. EMBO J. 16, 4163–4173.
Gajovic, S., St-Onge, L., Yokota, Y., Gruss, P., 1997. Retinoic acid mediates Pax6 expression during in vitro differentiation of embryonic stem cells. Differentiation 62, 187–192.
Galceran, J., Farinas, I., Depew, M.J., Clevers, H., Grosschedl, R., 1999. Wnt3a−/− like phenotype and limb deficiency in Lef1−/−Tcf1−/− mice. Genes Dev. 13, 709–717.
Gratsch, T.E., O'Shea, K.S., 2002. Noggin and chordin have distinct activities in promoting lineage commitment of mouse embryonic stem (ES) cells. Dev. Biol. 245, 83–94.
Helms, A.W., Johnson, J.E., 2003. Specification of dorsal spinal cord interneurons. Curr. Opin. Neurobiol. 13, 42–49.
Herrmann, B.G., Labeit, S., Poustka, A., King, T.R., Lehrach, H., 1990. Cloning of the T gene required in mesoderm formation in the mouse. Nature 343, 617–622.
Hitoshi, S., Tropepe, V., Ekker, M., van der Kooy, D., 2002. Neural stem cell lineages are regionally specified, but not committed, within distinct compartments of the developing brain. Development 129, 233–244.
Hooper, M., Hardy, K., Handyside, A., Hunter, S., Monk, M., 1987. HPRT-deficient (Lesch-Nyhan) mouse embryos derived from germline colonization by cultured cells. Nature 326, 292–295.
Horton, C., Maden, M., 1995. Endogenous distribution of retinoids during normal development and teratogenesis in the mouse embryo. Dev. Dyn. 202, 312–323.
Incardona, J., Gaffield, W., Kapur, R., Roelink, H., 1998. The teratogenic Veratrum alkaloid cyclopamine inhibits sonic hedgehog signal transduction. Development 125, 3553–3562.
Jensen, J., Serup, P., Karlsen, C., Nielsen, T.F., Madsen, O.D., 1996. mRNA profiling of rat islet tumors reveals Nkx 6.1as a beta -Cell-specific homeodomain transcription factor. J. Biol. Chem. 271, 18749–18758.
Jessell, T.M., 2000. Neuronal specification in the spinal cord: inductive signals and transcriptional codes. Nat. Rev., Genet. 1, 20–29.
Jonsson, J., Carlsson, L., Edlund, T., Edlund, H., 1994. Insulin-promoter-factor 1 is required for pancreas development in mice. Nature 371, 606–609.
Kawasaki, H., Mizuseki, K., Nishikawa, S., Kaneko, S., Kuwana, Y., Nakanishi, S., Nishikawa, S.I., Sasai, Y., 2000. Induction of midbrain dopaminergic neurons from ES cells by stromal cell-derived inducing activity. Neuron 28, 31–40.
Kawasaki, H., Suemori, H., Mizuseki, K., Watanabe, K., Urano, F., Ichinose, H., Haruta, M., Takahashi, M., Yoshikawa, K., Nishikawa, S., Nakatsuji, N., Sasai, Y., 2002. Generation of dopaminergic neurons and pigmented epithelia from primate ES cells by stromal cell-derived inducing activity. Proc. Natl. Acad. Sci. U. S. A. 99, 1580–1585.
Kessel, M., 1992. Respecification of vertebral identities by retinoic acid. Development 115, 487–501.
Kessel, M., Gruss, P., 1991. Homeotic transformations of murine vertebrae and concomitant alteration of Hox codes induced by retinoic acid. Cell 67, 89–104.
Kim, J.H., Auerbach, J.M., Rodriguez-Gomez, J.A., Velasco, I., Gavin, D., Lumelsky, N., Lee, S.H., Nguyen, J., Sanchez-Pernaute, R., Bankiewicz, K., McKay, R., 2002. Dopamine neurons derived from embryonic stem cells function in an animal model of Parkinson's disease. Nature 418, 50–56.
Knecht, A.K., Bronner-Fraser, M., 2002. Induction of the neural crest: a multigene process. Nat. Rev., Genet. 3, 453–461.
Kohtz, J.D., Lee, H.Y., Gaiano, N., Segal, J., Ng, E., Larson, T., Baker, D.P., Garber, E.A., Williams, K.P., Fishell, G., 2001. N-terminal fatty-acylation of sonic hedgehog enhances the induction of rodent ventral forebrain neurons. Development 128, 2351–2363.
Kohyama, J., Abe, H., Shimazaki, T., Koizumi, A., Okano, H., Hata, J., Umezawa, A., Nakashima, K., Taga, T., Gojo, S., 2001. Brain from bone: Efficient "meta-differentiation" of marrow stroma-derived mature osteoblasts to neurons with Noggin or a demethylating agent. Differentiation 68, 235–244.
Komuro, I., Izumo, S., 1993. Csx: a murine homeobox-containing gene specifically expressed in the developing heart. Proc. Natl. Acad. Sci. 90, 8145–8149.
Lee, S.H., Lumelsky, N., Studer, L., Auerbach, J.M., McKay, R.D., 2000. Efficient generation of midbrain and hindbrain neurons from mouse embryonic stem cells. Nat. Biotechnol. 18, 675–699.
Leonard, L., Horton, C., Maden, M., Pizzey, J.A., 1995. Anteriorization of CRABP-I expression by retinoic acid in the developing mouse central nervous system and its relationship to teratogenesis. Dev. Biol. 168, 514–528.
Lints, T., Parsons, L., Hartley, L., Lyons, I., Harvey, R., 1993. Nkx-2.5: a novel murine homeobox gene expressed in early heart progenitor cells and their myogenic descendants. Development 119, 419–431.
Liu, J.P., Laufer, E., Jessell, T.M., 2001. Assigning the positional identity of spinal motor neurons: rostrocaudal patterning of Hox-c expression by FGFs, Gdf11, and retinoids. Neuron 32, 997–1012.
Lu, Q.R., Yuk, D.-i., Alberta, J.A., Zhu, Z., Pawlitzky, I., Chan, J., McMahon, A.P., Stiles, C.D., Rowitch, D.H., 2000. Sonic hedgehog-regulated oligodendrocyte lineage genes encoding bHLH proteins in the mammalian central nervous system. Neuron 25, 317–329.
Maden, M., 2001. Role and distribution of retinoic acid during CNS development. Int. Rev. Cytol. 209, 1–77.
Maden, M., 2002. Retinoid signalling in the development of the central nervous system. Nat. Rev., Neurosci. 3, 843–853.
Maden, M., Horton, C., Graham, A., Leonard, L., Pizzey, J., Siegenthaler, G., Lumsden, A., Eriksson, U., 1992. Domains of cellular retinoic acid-binding protein I (CRABP I) expression in the hindbrain and neural crest of the mouse embryo. Mech. Dev. 37, 13–23.
Maden, M., Sonneveld, E., van der Saag, P., Gale, E., 1998. The distribution of endogenous retinoic acid in the chick embryo: implications for developmental mechanisms. Development 125, 4133–4144.
Marquardt, T., Pfaff, S.L., 2001. Cracking the transcriptional code for cell specification in the neural tube. Cell 106, 651–654.
Marshall, H., Nonchev, S., Sham, M.H., Muchamore, I., Lumsden, A., Krumlauf, R., 1992. Retinoic acid alters hindbrain Hox code and induces transformation of rhombomeres 2/3 into a 4/5 identity. Nature 360, 737–741.

Marti, E., Takada, R., Bumcrot, D., Sasaki, H., McMahon, A., 1995. Distribution of Sonic hedgehog peptides in the developing chick and mouse embryo. Development 121, 2537–2547.

Maye, P., Becker, S., Siemen, H., Thorne, J., Byrd, N., Carpentino, J., Grabel, L., 2004. Hedgehog signaling is required for the differentiation of ES cells into neurectoderm. Dev. Biol. 265, 276–290.

McGowan, K.M., Coulombe, P.A., 1998. Onset of keratin 17 expression coincides with the definition of major epithelial lineages during skin development. J. Cell Biol. 143, 469–486.

Mizuguchi, R., Sugimori, M., Takebayashi, H., Kosako, H., Nagao, M., Yoshida, S., Nabeshima, Y., Shimamura, K., Nakafuku, M., 2001. Combinatorial roles of olig2 and neurogenin2 in the coordinated induction of pan-neuronal and subtype-specific properties of motoneurons. Neuron 31, 757–771.

Mizuseki, K., Sakamoto, T., Watanabe, K., Muguruma, K., Ikeya, M., Nishiyama, A., Arakawa, A., Suemori, H., Nakatsuji, N., Kawasaki, H., Murakami, F., Sasai, Y., 2003. Generation of neural crest-derived peripheral neurons and floor plate cells from mouse and primate embryonic stem cells. Proc. Natl. Acad. Sci. U. S. A. 100, 5828–5833.

Muhr, J., Graziano, E., Wilson, S., Jessell, T.M., Edlund, T., 1999. Convergent inductive signals specify midbrain, hindbrain, and spinal cord identity in gastrula stage chick embryos. Neuron 23, 689–702.

Niederreither, K., Vermot, J., Schuhbaur, B., Chambon, P., Dolle, P., 2000. Retinoic acid synthesis and hindbrain patterning in the mouse embryo. Development 127, 75–85.

Niwa, H., Miyazaki, J., Smith, A.G., 2000. Quantitative expression of Oct-3/4 defines differentiation, dedifferentiation or self-renewal of ES cells. Nat. Genet. 24, 372–376.

Novitch, B.G., Chen, A.I., Jessell, T.M., 2001. Coordinate regulation of motor neuron subtype identity and pan-neuronal properties by the bHLH repressor Olig2. Neuron 31, 773–789.

Novitch, B.G., Wichterle, H., Jessell, T.M., Sockanathan, S., 2003. A requirement for retinoic acid-mediated transcriptional activation in ventral neural patterning and motor neuron specification. Neuron 40, 81–95.

Offield, M., Jetton, T., Labosky, P., Ray, M., Stein, R., Magnuson, M., Hogan, B., Wright, C., 1996. PDX-1 is required for pancreatic outgrowth and differentiation of the rostral duodenum. Development 122, 983–995.

Okabe, S., Forsberg-Nilsson, K., Spiro, A.C., Segal, M., McKay, R.D., 1996. Development of neuronal precursor cells and functional postmitotic neurons from embryonic stem cells in vitro. Mech. Dev. 59, 89–102.

Pattyn, A., Morin, X., Cremer, H., Goridis, C., Brunet, J., 1997. Expression and interactions of the two closely related homeobox genes Phox2a and Phox2b during neurogenesis. Development 124, 4065–4075.

Pattyn, A., Hirsch, M., Goridis, C., Brunet, J., 2000. Control of hindbrain motor neuron differentiation by the homeobox gene Phox2b. Development 127, 1349–1358.

Pevny, L.H., Sockanathan, S., Placzek, M., Lovell-Badge, R., 1998. A role for SOX1 in neural determination. Development 125, 1967–1978.

Pierani, A., Brenner-Morton, S., Chiang, C., Jessell, T.M., 1999. A sonic hedgehog-independent, retinoid-activated pathway of neurogenesis in the ventral spinal cord. Cell 97, 903–915.

Porter, J.A., von Kessler, D.P., Ekker, S.C., Young, K.E., Lee, J.J., Moses, K., Beachy, P.A., 1995. The product of hedgehog autoproteolytic cleavage active in local and long-range signalling. Nature 374, 363–366.

Porter, J.A., Ekker, S.C., Park, W.J., von Kessler, D.P., Young, K.E., Chen, C.H., Ma, Y., Woods, A.S., Cotter, R.J., Koonin, E.V., Beachy, P.A., 1996. Hedgehog patterning activity: role of a lipophilic modification mediated by the carboxy-terminal autoprocessing domain. Cell 86, 21–34.

Renoncourt, Y., Carroll, P., Filippi, P., Arce, V., Alonso, S., 1998. Neurons derived in vitro from ES cells express homeoproteins characteristic of motoneurons and interneurons. Mech. Dev. 79, 185–197.

Reynolds, K., Mezey, E., Zimmer, A., 1991. Activity of the beta-retinoic acid receptor promoter in transgenic mice. Mech. Dev. 36, 15–29.

Roelink, H., Porter, J.A., Chiang, C., Tanabe, Y., Chang, D.T., Beachy, P.A., Jessell, T.M., 1995. Floor plate and motor neuron induction by different concentrations of the amino-terminal cleavage product of sonic hedgehog autoproteolysis. Cell 81, 445–455.

Rohwedel, J., Guan, K., Wobus, A.M., 1999. Induction of cellular differentiation by retinoic acid in vitro. Cells Tissues Organs 165, 190–202.

Ross, S.A., McCaffery, P.J., Drager, U.C., De Luca, L.M., 2000. Retinoids in Embryonal Development. Physiol. Rev. 80, 1021–1054.

Ross, S.E., Greenberg, M.E., Stiles, C.D., 2003. Basic helix-loop-helix factors in cortical development. Neuron 39, 13–25.

Ruberte, E., Friederich, V., Chambon, P., Morriss-Kay, G., 1993. Retinoic acid receptors and cellular retinoid binding proteins: III. Their differential transcript distribution during mouse nervous system development. Development 118, 267–282.

Sakai, Y., Meno, C., Fujii, H., Nishino, J., Shiratori, H., Saijoh, Y., Rossant, J., Hamada, H., 2001. The retinoic acid-inactivating enzyme CYP26 is essential for establishing an uneven distribution of retinoic acid along the anterio-posterior axis within the mouse embryo. Genes Dev. 15, 213–225.

Schuurmans, C., Guillemot, F., 2002. Molecular mechanisms underlying cell fate specification in the developing telencephalon. Curr. Opin. Neurobiol. 12, 26–34.

Shimazaki, T., Shingo, T., Weiss, S., 2001. The ciliary neurotrophic factor/leukemia inhibitory factor/gp130 receptor complex operates in the maintenance of mammalian forebrain neural stem cells. J. Neurosci. 21, 7642–7653.

Sive, H.L., Draper, B.W., Harland, R.M., Weintraub, H., 1990. Identification of a retinoic acid-sensitive period during primary axis formation in *Xenopus laevis*. Genes Dev. 4, 932–942.

Smith, W.C., Harland, R.M., 1992. Expression cloning of noggin, a new dorsalizing factor localized to the Spemann organizer in *Xenopus* embryos. Cell 70, 829–840.

Sockanathan, S., Jessell, T.M., 1998. Motor neuron-derived retinoid signaling specifies the subtype identity of spinal motor neurons. Cell 94, 503–514.

Strubing, C., Ahnert-Hilger, G., Shan, J., Wiedenmann, B., Hescheler, J., Wobus, A.M., 1995. Differentiation of pluripotent embryonic stem cells into the neuronal lineage in vitro gives rise to mature inhibitory and excitatory neurons. Mech. Dev. 53, 275–287.

Swindell, E.C., Thaller, C., Sockanathan, S., Petkovich, M., Jessell, T.M., Eichele, G., 1999. Complementary domains of retinoic acid production and degradation in the early chick embryo. Dev. Biol. 216, 282–296.

Takebayashi, H., Yoshida, S., Sugimori, M., Kosako, H., Kominami, R., Nakafuku, M., Nabeshima, Y., 2000. Dynamic expression of basic helix-loop-helix Olig family members: implication of Olig2 in neuron and oligodendrocyte differentiation and identification of a new member, Olig3. Mech. Dev. 99, 143–148.

Temple, S., 2001. The development of neural stem cells. Nature 414, 112–117.

Tonegawa, A., Takahashi, Y., 1998. Somitogenesis controlled by noggin. Dev. Biol. 202, 172–182.

Tropepe, V., Hitoshi, S., Sirard, C., Mak, T.W., Rossant, J., van der Kooy, D., 2001. Direct neural fate specification from embryonic stem cells: a primitive mammalian neural stem cell stage acquired through a default mechanism. Neuron 30, 65–78.

Wagner, M., Han, B., Jessell, T., 1992. Regional differences in retinoid release from embryonic neural tissue detected by an in vitro reporter assay. Development 116, 55–66.

Wang, H.-F., Liu, F.-C., 2001. Developmental restriction of the LIM homeodomain transcription factor Islet-1 expression to cholinergic neurons in the rat striatum. Neuroscience 103, 999–1016.

Wichterle, H., Lieberam, I., Porter, J.A., Jessell, T.M., 2002. Directed differentiation of embryonic stem cells into motor neurons. Cell 110, 385–397.

Wilkinson, D.G., Bhatt, S., Herrmann, B.G., 1990. Expression pattern of the mouse T gene and its role in mesoderm formation. Nature 343, 657–659.

Wood, H.B., Episkopou, V., 1999. Comparative expression of the mouse Sox1, Sox2 and Sox3 genes from pre-gastrulation to early somite stages. Mech. Dev. 86, 197–201.

Wurst, W., Bally-Cuif, L., 2001. Neural plate patterning: upstream and downstream of the isthmic organizer. Nat. Rev. Neurosci. 2, 99–108.

Yamaguchi, T.P., Takada, S., Yoshikawa, Y., Wu, N., McMahon, A.P., 1999. T (Brachyury) is a direct target of Wnt3a during paraxial mesoderm specification. Genes Dev. 13, 3185–3190.

Ying, Q.L., Stavridis, M., Griffiths, D., Li, M., Smith, A., 2003. Conversion of embryonic stem cells into neuroectodermal precursors in adherent monoculture. Nat. Biotechnol. 21, 183–186.

Yoshikawa, Y., Fujimori, T., McMahon, A.P., Takada, S., 1997. Evidence that absence ofWnt-3aSignaling promotes neuralization instead of paraxial mesoderm development in the mouse. Dev. Biol. 183, 234–242.

Zhou, Q., Choi, G., Anderson, D.J., 2001. The bHLH transcription factor Olig2 promotes oligodendrocyte differentiation in collaboration with Nkx2.2. Neuron 31, 791–807.

Zimmer, A., 1992. Induction of a RAR beta 2-lacZ transgene by retinoic acid reflects the neuromeric organization of the central nervous system. Development 116, 977–983.

Zimmerman, L.B., De Jesus-Escobar, J.M., Harland, R.M., 1996. The Spemann organizer signal noggin binds and inactivates bone morphogenetic protein 4. Cell 86, 599–606.

Gene Expression Profile of Spinal Motor Neurons in Sporadic Amyotrophic Lateral Sclerosis

Yue-Mei Jiang, PhD,[1] Masahiko Yamamoto, MD,[1] Yasushi Kobayashi, MD,[1] Tsuyoshi Yoshihara, PhD,[1] Yideng Liang, PhD,[1] Shinichi Terao, MD,[2] Hideyuki Takeuchi, MD,[1] Shinsuke Ishigaki, MD,[1] Masahisa Katsuno, MD,[1] Hiroaki Adachi, MD,[1] Jun-ichi Niwa, MD,[1] Fumiaki Tanaka, MD,[1] Manabu Doyu, MD,[1] Mari Yoshida, MD,[3] Yoshio Hashizume, MD,[3] and Gen Sobue, MD[1]

The causative pathomechanism of sporadic amyotrophic lateral sclerosis (ALS) is not clearly understood. Using microarray technology combined with laser-captured microdissection, gene expression profiles of degenerating spinal motor neurons isolated from autopsied patients with sporadic ALS were examined. Gene expression was quantitatively assessed by real-time reverse transcription polymerase chain reaction and in situ hybridization. Spinal motor neurons showed a distinct gene expression profile from the whole spinal ventral horn. Three percent of genes examined were downregulated, and 1% were upregulated in motor neurons. Downregulated genes included those associated with cytoskeleton/axonal transport, transcription, and cell surface antigens/receptors, such as dynactin, microtubule-associated proteins, and early growth response 3 (EGR3). In contrast, cell death–associated genes were mostly upregulated. Promoters for cell death pathway, death receptor 5, cyclins A1 and C, and caspases-1, -3, and -9, were upregulated, whereas cell death inhibitors, acetyl-CoA transporter, and NF-κB were also upregulated. Moreover, neuroprotective neurotrophic factors such as ciliary neurotrophic factor (CNTF), Hepatocyte growth factor (HGF), and glial cell line–derived neurotrophic factor were upregulated. Inflammation-related genes, such as those belonging to the cytokine family, were not, however, significantly upregulated in either motor neurons or ventral horns. The motor neuron–specific gene expression profile in sporadic ALS can provide direct information on the genes leading to neurodegeneration and neuronal death and are helpful for developing new therapeutic strategies.

Ann Neurol 2005;57:236–251

Amyotrophic lateral sclerosis (ALS) is a devastating neurodegenerative disease characterized by loss of motor neurons in the spinal cord, brainstem, and motor cortex.[1] Initial symptoms include weakness of the limbs, abnormalities of speech, and difficulties in swallowing. The weakness ultimately progresses to complete paralysis, and half of the patients die within 3 years after the onset of symptoms, mostly because of respiratory failure. Approximately 10% of all ALS patients show familial traits, and 20 to 30% of familial ALS patients are associated with a mutation in the copper/zinc superoxide dismutase 1 gene (SOD1). However, more than 90% of ALS patients are sporadic, not showing any familial trait. The presence of Bunina bodies in the remaining spinal motor neurons is a hallmark of sporadic ALS cases.[2,3] So far, several hypotheses about the pathogenesis of sporadic ALS have been proposed based on extensive research on sporadic ALS: oxidative stress, glutamate excitotoxicity, impaired axonal transport, mitochondrial dysfunction, neurotrophic deprivation, proteasomal dysfunction, neuroinflammation, autoimmunity, viral infection, and others.[4–11] Nevertheless, the actual pathogenic mechanism of the selective motor neuron degeneration and ultimate cell death in sporadic ALS remains unknown. There have been extensive studies using animal models and culture systems for familial ALS, especially with SOD1 mutations, but no similar approach is available for studying sporadic ALS.

Recently advances in DNA microarray technology make it possible to analyze global gene expression profiles of thousands of genes in normal as well as pathological tissues. Global gene expression studies using DNA microarray technology have generated valuable

From the [1]Department of Neurology, Nagoya University Graduate School of Medicine, Nagoya; [2]Department of Internal Medicine, Aichi Medical University School of Medicine; and [3]Department of Neuropathology, Institute for Medical Science of Aging, Aichi Medical University School of Medicine, Nagakute, Aichi, Japan.

Received Sep 7, 2004, and in revised form Oct 22. Accepted for publication Nov 14, 2004.

Published online Jan 26, 2005, in Wiley InterScience (www.interscience.wiley.com). DOI: 10.1002/ana.20379

Address correspondence to Dr Sobue, Department of Neurology, Nagoya University Graduate School of Medicine, Nagoya 466-8550, Japan. E-mail: sobueg@med.nagoya-u.ac.jp

information about cell behavior in tissues consisting of homogeneous cell types, cultured cells, and cancer tissues of monoclonal origin.[12,13] In the case of neuronal tissues, particularly those of patients with neurological diseases, however, the complexity of tissues containing multiple lineages of cells, such as neurons, glial cells, and vascular tissues, places limitations on the use of DNA microarray technology. In the lesions of ALS spinal cords, there are reduced numbers of motor neurons with glial cell proliferation, making it difficult to examine motor neuron–specific gene expression.

Laser-captured microdissection (LCM) has been reported to make it possible to isolate single individual neurons from neural tissues with well-preserved mRNA quality.[14,15] In addition, RNA amplification techniques preserving the relative amounts of individual mRNAs have been developed recently.[16,17] LCM and RNA amplification combined with DNA microarray analyses have been reported to enable studies of cell type–specific gene expression profiles in tissues with multiple cell lineages.[16,18] Such integrated analysis system provide an effective tool for investigating the cellular events affecting cell type–specific gene expression profiles in neurodegenerative diseases such as ALS. Indeed, we and other groups demonstrated that these integrated systems could be applied successfully to describe cell-specific gene expression profiles in neuronal tissues.[15,18]

In this study, we applied integrated LCM, RNA amplification, and DNA microarray analysis to clarify alterations of motor neuron–specific gene expression in sporadic ALS cases and successfully obtained expression gene database in situ from degenerating motor neurons in sporadic ALS spinal cord.

Patients and Methods

Tissues from Amyotrophic Lateral Sclerosis and Control Patients

Fresh specimens of lumbar spinal cord (L4 to L5 segment) from 14 sporadic ALS patients (nine men, five women) and 13 neurologically normal patients (nine men, four women) were obtained at autopsy (Table 1). Diagnosis of ALS was

Table 1. Details of Patients Examined in This Study

Patients	Sex	Age (yr)	Duration of Illness (yr)	Postmortem Delay (hr)	Diseases	Spinal Cord Neuropathology Motor Neuron Loss/Gliosis
ALS1	M	72	3.7	6	ALS (B, UL, LL)	Moderate/mild
ALS2	M	71	2.3	5	ALS (LL, UL)	Moderate/mild
ALS3	M	58	1.8	13	ALS (UL, LL, B)	Severe/severe
ALS4	M	43	2.6	5	ALS (LL, B)	Moderate/mild
ALS5	M	53	2.8	11	ALS (B, UL, LL)	Moderate/severe
ALS6	F	79	4.0	4	ALS (UL, LL, B)	Severe/severe
ALS7	F	59	2.5	3	ALS (UL)	Mild/mild
ALS8	F	67	2.0	7	ALS (UL, B)	Severe/mild
ALS9	M	74	4.3	10	ALS (LL, B)	Severe/mild
ALS10	F	47	1.8	4	ALS (B, UL, LL)	Mild/mild
ALS11	M	74	4.5	12	ALS (UL, LL)	Moderate/mild
ALS12	M	57	3.5	5	ALS (LL, UL)	Severe/mild
ALS13	F	53	3.0	8	ALS (B, UL, LL)	Severe/severe
ALS14	M	63	2.2	5	ALS (UL, B)	Mild/mild
Control1	M	57	—	7	Pneumonia	No
Control2	M	78	—	10	Cerebral infarction	No
Control3	M	72	—	9	Lung cancer	No
Control4	F	52	—	7	Pneumonia	No
Control5	F	65	—	12	Pneumonia	No
Control6	M	75	—	10	Heart failure	No
Control7	M	42	—	5	Heart failure	No
Control8	F	76	—	5	Pancreas cancer	No
Control9	F	84	—	6	Myocardial infarction	No
Control10	M	48	—	13	Heart failure	No
Control11	M	77	—	11	Heart failure	No
Control12	M	66	—	11	Cerebral infarction	No
Control13	M	75	—	4	Pneumonia	No

The age, duration of illness, and postmortem delay are indicated for the ALS and control cases. Predominant clinical features of ALS are shown: UL = upper limbs; LL = lower limbs; B = bulbar. Neuropathological involvement of spinal cords was graded as previously. Ten ALS samples were used for microarray analysis: five of them (1, 7, 10, 11, and 14) were analyzed using 4.8K array for spinal motor neurons; five (2, 4, 5, 8, and 12) using 1.0K for spinal motor neurons; five (1, 3, 10, 13, and 14) using 4.8K for spinal ventral horn gray matter; and five (1, 2, 4, 5, and 13) and five (1, 2, 7, 8, and 10) control samples using 4.8K and 1.0K. Thirteen ALS (1–13) and 11 (1–11) control samples were used for TaqMan reverse transcription polymerase chain reaction analysis. Five ALS (1, 10, 11, 13, and 14) and four control (1, 3, 5, and 12) samples were used for in situ hybridization and immunohistochemistry.
ALS = amyotrophic lateral sclerosis.

confirmed by El Escorial diagnostic criteria defined by the World Federation of Neurology and the histopathological findings, particularly the presence of the Bunina body.[2,3] All cases of ALS were sporadic and did not show any heredity. ALS patients with *SOD1* mutation were excluded. The collection of tissues and their use for this study were approved by the ethics committee of Nagoya University Graduate School of Medicine. Tissues were frozen immediately and stored at −80°C until use. The mean ages and standard deviations for ALS and control patients were 62.1 ± 11.0 and 66.7 ± 13.1 years, and the mean postmortem intervals and standard deviations were 7.0 ± 3.3 and 8.5 ± 3.0 hours, respectively. The differences between the means of either age or postmortem interval were not significant between the ALS and control groups. The cause of death in all ALS patients was respiratory failure, and the causes in the control patients were pneumonia, lung cancer, or acute heart failure (see Table 1). Parts of the lumbar spinal cord were fixed in 10% buffered formalin solution, and processed for paraffin sections. The sections were stained with hematoxylin and eosin and Klüver-Barrera and Holzer techniques, and histological assessment was performed. The degree of motor neuron loss and astrogliosis was ranked as mild, moderate or severe according to previously reported.[19,20]

Laser-Captured Microdissection of Spinal Motor Neurons

Sections (10μm) were cut with a standard cryostat, mounted on poly-L-lysin coated slides (Zeiss, Thornwood, NY), and stained with hematoxylin to identify the motor neurons located in the medial and lateral nuclei of the ventral horns of lumber spinal cords. After staining with hematoxylin, the sections were washed in RNase-free water and dried.[21,22] The PALM Robot-Microbeam system (P.A.L.M. Mikrolaser Technology AG, Bernried, Germany) was used for laser capture. The pulsed laser microbeam cut precisely around the targeted motor neurons in the spinal ventral horn (LCM; see Fig 1A–C). The identity of motor neurons was ascertained by reverse transcription polymerase chain reaction (RT-PCR) for choline acetyltransferase (ChAT) as described previously.[15] Each laser-isolated specimen subsequently was ejected from the glass slide with a single or several laser shots and collected directly into the cap of a PCR tube containing denaturing buffer by a process of laser pressure catapulting in the totally noncontact manner previously described.[23] The LCM-isolated cells (approximately 500 pooled cells) were dissolved in denaturing buffer (StrataPrep Total RNA Microprep Kit; Stratagene, San Diego, CA) and stored at −80°C until use.

RNA Extraction of Laser-Captured Microdissection Motor Neuron Samples and Spinal Ventral Horn Homogenates

LCM-isolated cells in denaturing buffer were thawed and centrifuged briefly before the RNA was extracted using a StrataPrep Total RNA Microprep Kit (Stratagene) according to the manufacturer's protocol. RNA was extracted as well from the total homogenates of ventral horn gray matter of spinal cords,[19] which was dissected under a dissecting microscope.

Reverse Transcription and T7 RNA Polymerase Amplification of RNA

Ten microliters of purified RNA obtained as described above was mixed with 1μl of 0.5μg/ml T7-oligodT primer (5′-TCTAGTCGACGGCCAGTGAATTGTAATACGACTCACTATAGGGCGT$_{21}$-3′) to initiate first-strand synthesis. The primer and RNA were incubated in 4μl of 5 × first-strand reaction buffer, 0.1M DTT (2μl), 10mM dNTPs (1μl), 1μl of RNasin, and 1μl of Superscript II reverse transcriptase (Invitrogen, Carlsbad, CA) at 42°C for 1 hour, and then 30μl of 5 × second-strand synthesis buffer, 10mM dNTPs (3μl), 4μl of DNA polymerase, 1μl of *Escherichia coli* RNase H, and 1μl of *E. coli* DNA ligase and 91μl of RNase-free H_2O were added, and the mixture was incubated at 16°C for 2 hours and then at 16°C for 10 minutes after the addition of 2μl of T4 DNA polymerase. Next, an Ampliscribe T7 Transcription Kit (Epicentre Technologies, Madison, WI) was used for RNA amplification: 8μl double-stranded cDNA, 2μl of 10 × Ampliscribe T7 buffer, 1.5μl each of 100mM ATP, CTP, GTP, and UTP, 0.1 M DTT (2μl), and 2μl of T7 RNA polymerase were incubated at 42°C for 3 hours.

For second-round amplification, 10μl of amplified RNA (aRNA) from first-round amplification was mixed together with 1μl of 1mg/ml random hexamers (Invitrogen), and then first-stranded cDNA was synthesized, followed by second-stranded cDNA synthesis as described above. The double-stranded cDNA was subjected to second-round T7 in vitro transcription as above and then subsequent third-round aRNA amplification. After third-round amplification, aRNA was treated with DNase (Wako, Kanagawa, Japan) and cleaned up using an RNeasy Kit (Qiagen, Valencia, CA) according to the manufacturer's protocol.

DNA Microarray Analysis

Fluorescent cDNA probes were synthesized from aRNA of laser-captured spinal motor neurons and RNA from ventral spinal tissue homogenates using an Atlas Glass Fluorescent Labeling Kit (Clontech, Palo Alto, CA) according to the manufacturer's protocol. Cy3-labeled cDNA probes were synthesized from ALS samples for spinal motor neurons and homogenates, and Cy5-labeled cDNA probes were synthesized from control samples. BD Atlas Glass Microarray Human 1.0 and 3.8 (Clontech) slides were hybridized with these fluorescent labeled probes overnight at 50°C and then washed four times and dried according to the manufacturer's protocol. Individual Cy3-labeled cDNA probes from ALS RNA samples of spinal motor neurons and homogenates for each patient were coupled with Cy5-labeled cDNA probes from control RNA samples of those tissues, which were prepared by mixing equal amounts of RNA samples amplified from the control patients. The microarrays were scanned in a laser scanner (GenePix 4000; Axon Instruments, Union City, CA), and the resulting signals were quantified and stored using GenePix Pro analysis software (Axon Instruments). The data for each expressed gene obtained from microarray analysis were expressed as the ratios of the values of individual ALS patients or the means of the values of ALS to the values of the control patients. The values of gene expression levels were means-calculated from motor neurons of 5 or 10 inde-

pendent individuals with ALS as well as from spinal ventral horns of 5 individuals with ALS.

Quantitative Real-Time Reverse Transcription Polymerase Chain Reaction

The probe and primers for the real-time PCR were designed using Primer3' (S. Rozen and H. J. Skaletsky, available at http://www-genome.wi.mit.edu/genome_software/other/primer3.html). TaqMan PCR was conducted using an iCycler system (Bio-Rad Laboratories, Hercules, CA) with a QuantiTect Probe PCR Kit (Qiagen) and the cDNA according to the manufacturer's protocol. The reaction conditions were 95°C for 3 minutes and then 50 cycles of 15 seconds at 95°C followed by 60 seconds at 55°C. All experiments were performed in quadruplicate, and several negative controls were included. For an internal standard control, the expression of glyceraldehyde-3-phosphate dehydrogenase (GAPDH) was simultaneously quantified. The primers and probe sequences for the examined genes (acetyl-CoA transporter: D88152; Bak: NM_001188; CRABP1: NM_004378; cyclin C: M74091; dynactin 1: NM_004082; EGR3: NM_004430; ephrin A1: M57730; GAPDH: NM_002046; KIAA0231: D86984; and TrkC: U05012) were described in the legends for Figure 3. The threshold cycles of each gene were determined as the number of PCR cycles at which the increase in reporter fluorescence reached 10 times above the baseline signal. The weight ratio of the target gene to GAPDH gives the standardized expression level.

In Situ Hybridization

Frozen sections (10μm thick) of the spinal cord were prepared and immediately fixed in 4% paraformaldehyde. Then, they were treated with 0.1% diethylpyrocarbonate (DEPC) twice for 15 minutes and prehybridized at 45°C for 1 hour. Digoxigenin-labeled cRNA probes were generated from linearized plasmids for the genes of interest using SP6 or T7 polymerase (Roche Diagnostics, Basel, Switzerland). Gene names, Genebank accession number, probe position (nucleotide number), and probe size were as follows: acetyl-CoA transporter, D88152, nucleotides 397-741, 345bp; Bak, NM_001188, nucleotides 792–2094, 345bp; CRABP1, NM_004378, nucleotides 210–545, 336bp; dynactin 1, NM_004082, nucleotides 2392–2774, 383bp; DR5, NM_004082, nucleotides 682–1070, 389bp; EGR3, NM_004430, nucleotides 1433–1794, 362bp; KIAA0231, D86984, nucleotides 698–1053, 356bp; TrkC, U05012, nucleotides 1412–1721, 310bp. After prehybridization, the sections were hybridized with each digoxigenin-labeled cRNA probe overnight at 45°C. The washed sections were incubated with alkaline phosphatase-conjugated anti–digoxigenin antibody (Roche Diagnostics). The signal was visualized with NBT/BCIP (Roche Diagnostics).

Immunohistochemistry

Frozen sections (10μm thick) of the spinal cord were prepared and immediately fixed in 4% paraformaldehyde. Then, they were blocked with 2% bovine serum albumin (Sigma) in Tris-buffered saline at room temperature for 20 minutes and incubated with anti–cyclin C (1:200 dilution; Santa Cruz Biotechnology, Santa Cruz, CA) antibody overnight at 4°C. Subsequent procedures were performed using ENVISION++KIT/HRP (diaminobenzidine tetrahydrochloride; DAKO, Carpinteria, CA) according to the manufacturer's protocol.

Statistical Analyses

To assess the correlation of intensity values for each labeling sample, we used scatterplots and measured linear relationships. The correlation coefficient, R^2, that was calculated indicates the variability of intensity values between Cy-5– and Cy-3–labeled samples. To perform cluster analyses of hierarchical clustering, self-organizing maps (SOM) and principal component analysis after logarithmic transformation, we used Acuity 3.0 software (Axon Instruments). The data measured by quantitative real-time RT-PCR analysis were analyzed by Student's t tests.

Results

T7 Amplification Preserves Gene Expression Profiles

Because the amounts of laser-microdissected samples were extremely low and did not contain enough mRNA for further analysis, RNA amplification was required. It was critical to achieve sufficient RNA amplification and yet maintain the expression profiles of mRNAs. We performed experiments to determine how the expression profiles of mRNAs were affected by the T7 amplification procedure. RNA samples were extracted from control spinal cords and a part of RNA samples was amplified using T7 amplification. One flourescently labeled probe was synthesized from an individually amplified RNA (aRNA) or nonamplified RNA (nRNA) and was hybridized to microarrays. Independent amplification of RNA yielded quite similar expression patterns. The correlation of signal intensities between independent amplifications for the third aRNA was $R^2 = 0.9157$, $p < 0.0001$, and on the other hand, the correlation of signal intensities in nRNA was $R^2 = 0.9157$, $p < 0.0001$ (Fig 1D, E). Previous reports using similar amplification procedures as ours also have confirmed the reproducibility of T7 amplification for the preservation of RNA expression profiles.[14,15,17] In this study, the third-round amplification was performed for the LCM-isolated motor neurons, but for the spinal ventral horn homogenates a single amplification produced enough RNA for further analysis, and similar expression patterns were found between the first and third amplifications (data not shown).

Gene Expression Database of Spinal Motor Neurons and Ventral Horn Homogenates of Amyotrophic Lateral Sclerosis

aRNA samples from the motor neurons and the ventral horn homogenates from the lumbar spinal cords were subjected to microarray analysis. The differences of the gene expression levels between ALS and control sam-

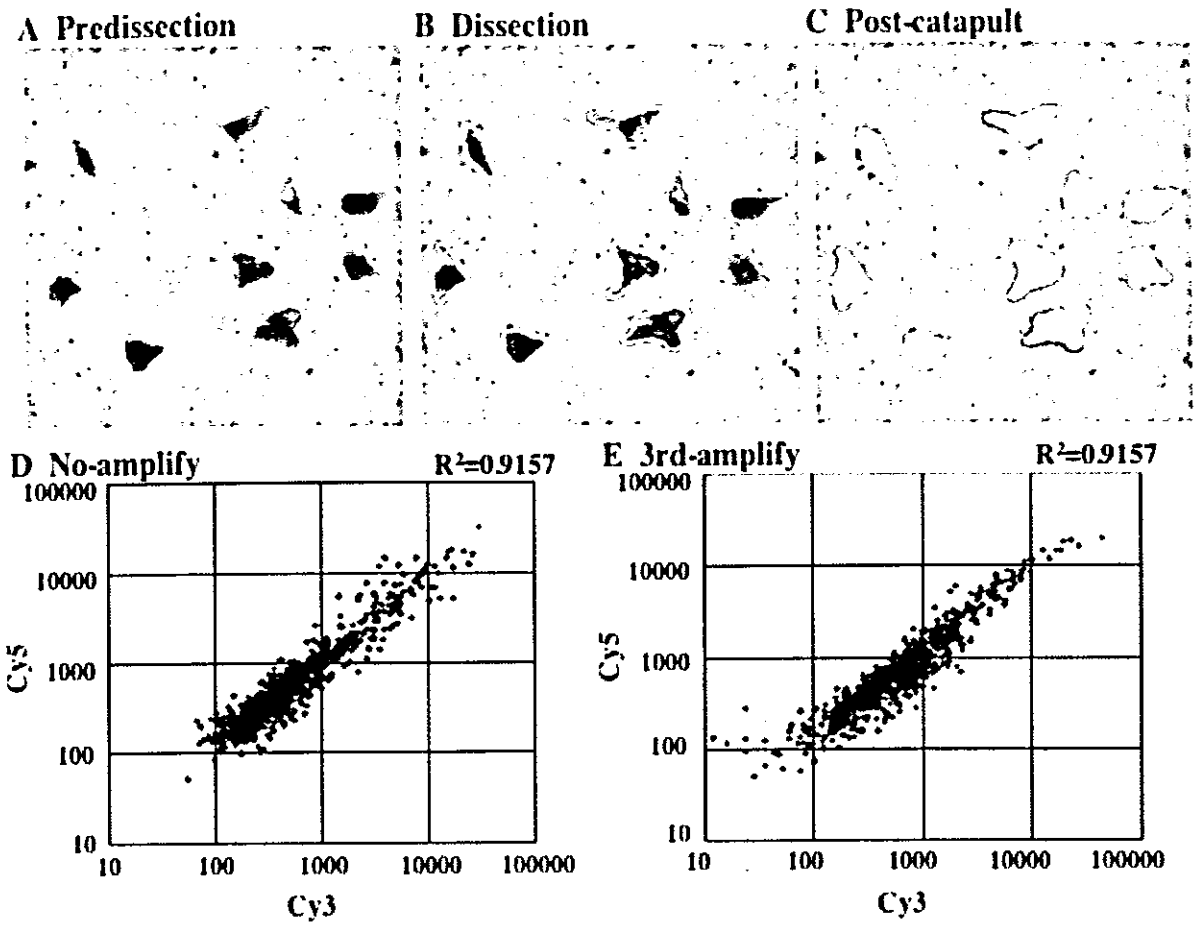

Fig 1. Verification of laser-captured microdissection (LCM) and RNA amplification. Microdissection of motor neurons in spinal ventral horn: sections were stained with hematoxylin (A); margins of motor neurons were dissected by the laser beam (B); and motor neurons were isolated from slides by laser pressure catapulting (C). Scatterplots of nonamplified and amplified RNAs: correlations between independent amplifications of control spinal cord samples are shown using nonamplified (D) and third amplified RNAs (E). These RNAs were split into two samples for labeling of Cy5 and Cy3 and hybridized separately to two microarrays. The very high squared correlations reflect the high reproducibility of the hybridization results with the same values between nonamplified and third amplified RNAs.

ples were expressed as ratios of the values of ALS individuals compared with the mean values of the controls. One percent (52/4,845) of genes examined were significantly upregulated in spinal motor neurons of ALS patients and 3% (144/4,845) were downregulated, assuming that the changes of 3.0-fold increase and 0.3-fold decrease were significant, when the mean levels of gene expression were calculated. In contrast with motor neurons, the total spinal ventral horn homogenates demonstrated 0.7% (37/4,845) and 0.2% (8/4,845) significant upregulation and downregulation of gene expression, respectively.

The genes prominently altered in ALS are listed in Tables 2 to 5 for spinal motor neurons and spinal ventral horn homogenates, respectively. Several upregulated genes listed were overlapping between spinal motor neurons (see Table 2) and ventral horns (see Table 4), suggesting that motor neuron overexpression is reflected to some extent by gene expression in ventral horn homogenates. The other genes upregulated in motor neurons were not present in the list for spinal ventral horns, because these gene expression changes were diluted and masked by changes occurring in other cell types. Because the number of spinal motor neurons was decreased in ALS spinal cords, most genes that were listed as downregulated genes in motor neurons (see Table 3) were not found in spinal ventral horns (see Table 5) except for three genes (CRABP1, EGR3, and postmeiotic segregation increased 2-like 11). When we categorized these altered genes in ALS motor neurons into several functional groups, the genes related to cell receptors and intracellular signaling, transcription,